A NUCLEAR MAGNETIC RESONANCE STUDY OF THE COMPLEXATION OF 23Na + BY 2-2-2 CRYPTAND

Thesis for the Degree of M. S. MICHIGAN STATE UNIVERSITY PATRICK B. SMITH 1977

LIBRILLY
Michigan State
University

., ≥,

A NUCLEAR MAGNETIC RESONANCE STUDY OF THE COMPLEXATION OF ²³Na⁺ BY

2-2-2 CRYPTAND

By

Patrick B. Smith

An investigation of the complexation of ²³Na⁺ by 2-2-2 cryptand in several solvents has been initiated. The chemical shifts and linewidths of the complexed and solvated ions have been measured by ²³Na NMR. Rate studies have also been performed on the exchange of Na⁺ between the two sites in four solvents; water, pyridine, tetrahydrofuran (THF), and ethylenediamine (EDA). It has been found that the solvent has a definite influence, not only on the solvated sodium ion but also on the complexed ion. The chemical shift of this species ranges from 9.2 ppm in water to 13.4 ppm in dimethylformamide. The kinetics of exchange is also very solvent dependent. The activation energy in Kcal mole⁻¹ for the dissociation step in water is 16.7, in THF it is 14.4, in pyridine it is 14.2 and in EDA it is 13.0.

A NUCLEAR MAGNETIC RESONANCE STUDY OF THE COMPLEXATION OF ²³Na⁺ BY 2-2-2 CRYPTAND

Ву

Patrick B. Smith

A THESIS

Submitted to
Michigan State University
in partial fulfillment of the requirements
for the degree of

MASTER OF SCIENCE

Department of Chemistry

1977

To my family

ACKNOWLEDGEMENTS

The author wishes to express gratitude to Professor James L.

Dye for his encouragement and guidance throughout this work.

Professor Alexander I. Popov is also gratefully acknowledged for his counseling.

The author would also like to acknowledge Dr. Joseph M. Ceraso for his many hours of instruction, encouragement and friendship.

Special appreciation also goes to Dr. David Wright for his many hours of valuable assistance. Mr. Timothy Kelly is also acknowledged for his help in computer programming and Mr. Stephen Landers for much of the linewidth data in this thesis.

A high degree of respect and appreciation are extended to Dr.

Elizabeth Mei, Mr. Michael Yemen, Mr. Michael DaGue, Mr. Charles

Andrews, Dr. Guan Huei Ho and Dr. Yves Cahen for many helpful

discussions in the laboratory. Financial support from the United States

Atomic Energy Commission is also acknowledged.

Lastly, my heart-felt appreciation is extended to my wife and family for their encouragement and love which has made the attainment of this goal possible.

TABLE OF CONTENTS

Chapte	er	Page
I.	INTRODUCTION	1
II.	HISTORICAL	
	THE NATURE OF INTERACTIONS IN SOLUTION	2
	EFFECTS INFLUENCING THE EXTENT OF INTERACTION	4
	MATHEMATICAL FORMULATION OF THE NMR RATE EXPERIMENT	5
	ALKALI METAL RATE STUDIES	8
III.	EXPERIMENTAL	
	GLASSWARE CLEANING	11
	SOLVENT PURIFICATION	11
	CHEMICAL PURIFICATION	11
	SAMPLE PREPARATION	11
	INSTRUMENTATION	11
	Super Con	11 12
IV.	RESULTS	
	THE NON-EXCHANGING SYSTEM	14
	THE EXCHANGING CASE	15
	SUSCEPTIBILITY OF ETHYL AMINE	27
v.	CONCLUSIONS	46
VI.	LITERATURE CITED	50
WTT	APDFNDTY	52

LIST OF TABLES

Tabl	е
1.	The Chemical Shift of ²³ Na in Several Solvents
2.	The Variation of the Linewidth and Chemical Shift of the Complexed and Free Na Cation with Temperature in EDA18
3.	The Variation of the Linewidth and Chemical Shift of the Complexed and Free 23Na Cation with Temperature in THF 19
4.	The Variation of the Linewidth and Chemical Shift of the Complexed and Free Na Cation with Temperature in Pyridine . 20
5.	The Variation of the Linewidth and Chemical Shift of the Complexed and Free Na Cation with Temperature in Water 22
6.	The Temperature Dependence of the Exchange Time and Linewidth in EDA
7.	The Temperature Dependence of the Exchange Time and Linewidth in THF
8.	The Temperature Dependence of the Exchange Time and Linewidth in Pyridine
9.	The Temperature Dependence of the Exchange Time and Linewidth in Water
10.	The Solvent Dependence of the Thermodynamic Parameters

LIST OF FIGURES

Figu	re
1.	Dibenzo-18-crown-6
2.	2-2-2 Crypt Used for the Complexation of ²³ Na
3.	Block Diagram of DA-60
4.	Block Diagram of the Lock System
5.	Space Diagram of the Complexed ²³ Na Cation
6.	The Variation of T ₂ with 1/T for EDA
7.	The Variation of T ₂ with 1/T for THF
8.	The Variation of T_2 with $1/T$ for Pyridine
9•	The Variation of T ₂ with 1/T for Water
10.	Typical Spectra Illustrating the 23Na NNR Lineshape for EDA 28
11.	Typical Spectra Illustrating the ²³ Na NMR Lineshape for THF 29
12.	Typical Spectra Illustrating the ²³ Na NMR Lineshape for Pyridine
13.	Typical Spectra Illustrating the ²³ Na NMR Lineshape for Water. 31
14.	A Typical KINFIT Analysis of the 23 Na Lineshape in EDA 32
15.	A Typical KINFIT Analysis of the 23 Na Lineshape in THF 33
16.	A Typical KINFIT Analysis of the ²³ Na Lineshape in Pyridine 34
17.	A Typical KINFIT Analysis of the 23 Na Lineshape in Water 35
18.	The Variation of the Log of k with the Inverse of the Temperature in EDA
19.	The Variation of the Log of k with the Inverse of the Temperature in THF
20.	The Variation of the Log of k with the Inverse of the Temperature in Pyridine
21.	The Variation of the Log of k with the Inverse of the Temperature in Water

LIST OF NOMENCLATURE, ABBREVIATIONS AND SYMBOLS

EDA: Ethylenediamine

THF: Tetrahydrofuran

DMF: Dimethylformamide

DMSO: Dimethylsulfoxide

NaTPB: Sodium Tetraphenylborate

 $\Delta v_{1/2}$ = Full width at half height

 ω = Chemical shift

 T_2 = Spin-spin relaxation time

 τ_A = Mean lifetime at site A

 τ = Exchange time = $\frac{\tau_A \tau_B}{\tau_A + \tau_B}$

 p_A = Population at site A

INTRODUCTION

CHAPTER I

Recent work in this laboratory has concentrated on the production and identification of alkali metal anions (23). Cryptands, which selectively complex alkali metal cations in solution have provided one means by which these species are produced in relatively high concentration. Cryptands are the best alkali cation complexing agents to date, yielding such tightly bound complexes (cryptates) that rate studies can be done on these systems. This project, in continuation of the preliminary rate study of Ceraso and Dye (16), has further investigated the solvent dependence of this exchange phenomenon as well as the solvent dependence of the chemical shift and linewidth of the complexed sodium cation.

CHAPTER II

HISTORICAL

THE NATURE OF INTERACTIONS OF ALKALI METALS IN SOLUTION

In the past, alkali metal nuclear magnetic resonance has afforded only two parameters to observers; linewidth and the chemical shift. Unlike proton NMR, where specific interactions are long lived, no fine structure is observed due to the extreme lability of these metal cations in solution. In order for a particular interaction to be observed on the NMR time scale, the ion must remain in a certain environment for about a millisecond or longer. If however, the ion moves rapidly throughout the solution experiencing many environments during this time period, then the effect of these environments will be averaged into a single absorption.

Although only two parameters may normally be obtained in alkali metal NMR, considerable information is provided by them. The chemical shift and linewidth both provide information concerning the nature, extent and lifetime of interactions in solution. The linewidth is related to T_2 , the spin-spin relaxation time by

$$T_2 = \frac{1}{\pi \Delta v_{l_s}} \tag{1}$$

where $\Delta v_{3/2}$ is the full width at half height in Hz, of a Lorentzian line. Since 23 Na has an appreciable quadrupole moment, its relaxation is dominated by the interaction of the quadrupole with electrostatic field gradients at the nucleus. Interactions with species which produce field gradients at the nucleus will be observed in line broadening. The extent of line broadening is useful in determining the geometry of the environment and the strength of the interaction.

These interactions affect the chemical shift in much the same

fashion since it is a measure of the shielding of the nucleus by the electrons around it. Since the field which the nucleus experiences is largely dependent upon the electronic shielding, any interaction which alters the character of these electronic orbitals will cause resonance to occur at higher or lower fields.

The chemical shift, relative to the bare nucleus, is made up of two components, a diamagnetic part, σ_d and a paramagnetic part, σ_p . σ_d is usually the larger of the two and arises mainly from the electronic distribution in the ground state. It is not strongly affected however by the environment of the ion. On the other hand, σ_p depends also on excited states through the mechanism of spin-orbit coupling. Interactions in solution have large effects on σ_p because solvent molecules and counter-ions tend to interact with valence electrons via unoccupied orbitals. Paramagnetic shifts are downfield whereas diamagnetic shifts are upfield.

There are several mechanisms by which interactions in solution are produced, the more important being 1) polarization of electronic orbitals by dipoles or ions, 2) ring currents from neighboring molecules and 3) donation of electrons from one species into the p-orbitals of another. Deverell and Richards (1) have undertaken a study in which they varied several parameters such as concentration, the cation or anion of various salts, etc., in order to determine which mechanism produced the greatest effects in solution. They observed that the concentration of cations and anions in solution had a definite influence on the chemical shift. They also noticed that some ions had larger effects on the counter ions than others, in fact that those with the greatest size and lowest charges tended to produce the greatest effect. From this,

they concluded that the major contributor to interactions was not due to polarization but was instead produced by donation of electrons into the p-orbitals of the counter ion, exciting those p-electrons to higher states.

EFFECTS INFLUENCING THE EXTENT OF INTERACTION

There are three major effects which govern the character of interactions of metal cations in solution in a given solvent. The anion produces the largest effect in that collisions of cation and anion produce excitation of ground state electrons as discussed earlier. As the concentration of the anion is increased, the frequency of collision is also increased, yielding greater effects (2-5).

The temperature also influences the linewidth, most obviosly because of solvent viscosity. Also however, as the temperature is decreased, the rate of exchange between sites is slowed down, producing longer lived interactions.

Thirdly, although the solvent interacts directly with the cation, another important effect on T₂ and the chemical shift is of a more subtle nature. The solvent controls the extent of dissociation of the salt so that it may be either conducive to ion pairing or it may solvate the ions very well so as to limit interaction between them. There is an entire spectrum of solvents ranging from those conducive to contact ion pairing, to those in which solvent-shared or solvent-separated ion pairs exist, and finally to those which prohibit ion pairing. Considerable documentation (2-7) has been recorded for these systems; and of particular interest to this discussion is the work of Popov and co-workers (2-3), in which they relate the Gutmann donor number of the solvent (which is a measure of its solvating ability) to

the chemical shift of ²³Na in that solvent. They found a linear relationship between the two.

MATHEMATICAL FORMULATION OF THE NMR RATE EXPERIMENT

If the exchange of a species from one environment to another is slow, NMR may be utilized to distinguish between a nucleus in site A and in site B; that is, two separate absorptions will occur. If on the other hand, the lifetime at a site is less than about 10⁻³ seconds, only one absorption will occur (an average of the two) because the sampling rate of the instrument is not rapid enough to "see" the nucleus in the two separate environments. The classical equations which govern NMR rate processes are the Bloch equations modified by McConnell (8) for exchange. We begin with the Bloch equations in the rotating frame

$$\frac{du}{dt} + \frac{u}{T_2} + (\omega_0 - \omega)v = 0$$
 (2)

$$\frac{d\mathbf{v}}{dt} + \frac{\mathbf{v}}{T_2} - (\omega_0 - \omega)\mathbf{u} + \gamma \mathbf{H}_1 \mathbf{M}_z = 0$$
 (3)

$$\frac{dM_z}{dt} + \frac{M_z - M_0}{T_1} - \gamma H_1 v = 0$$
 (4)

where

$$M_x = u \cos \omega t - v \sin \omega t$$
 (5)

$$M_y = -v \cos \omega t - u \sin \omega t$$
 (6)

If we define a complex moment

$$G = u + iv \tag{7}$$

then equations 1-3 become

$$\frac{dG}{dt} + \left[\frac{1}{T_2} - i(\omega_0 - \omega)\right]G = -i\gamma H_1 M_0$$
 (8)

This equation governs the behavior of a system when all nuclei therein experience the same magnetic environment. If instead, a system contains two magnetic environments, there will be two independent macroscopic moments. If no exchange of nuclei occurs between sites A and B we have

$$\frac{dG_{A}}{dt} + \left[\frac{1}{T_{2A}} - i(\omega_{OA} - \omega)\right] G_{A} = -i\gamma H_{1}M_{OA}$$
 (9)

$$\frac{dG_B}{dt} + \left[\frac{1}{T_{2B}} - i(\omega_{OB} - \omega)\right]G_B = -i\gamma H_1 M_{OB}$$
 (10)

These equations must be further modified to take account of exchange between sites A and B. If we define τ_A and τ_B as the mean lifetime of a nucleus in sites A and B respectively, and assume that nuclei jump directly from one site to another with no intermediate states involved, we may write

$$\frac{dG_A}{dt} + \alpha_A G_A = -i\gamma H_1 M_{OA} + \tau_B^{-1} G_B - \tau_A^{-1} G_A$$
 (11)

$$\frac{dG_B}{DT} + \alpha_B G_B = -i \gamma H_1 M_{OA} + \tau_A^{-1} G_A - \tau_B^{-1} G_B$$
 (12)

where G_B/τ_B is the rate of increase of G_A due to chemical transfer of magnetization from the B system to the A system and $-G_A/\tau_A$ is the rate of decrease in G_A due to chemical transfer of magnetization from system A to system B, and

$$\alpha_{\mathbf{A}} = \frac{1}{T_{2\mathbf{A}}} - \mathbf{i} \left(\omega_{\mathbf{O}\mathbf{A}} - \omega \right) \tag{13}$$

In order to solve these differential equations, we invoke the "slow passage condition", which states that if we scan the frequency slowly enough so as not to perturb the system's thermal equilibrium, we may assert that

$$\frac{dG_A}{dt} = \frac{dG}{dt}B = 0 \tag{14}$$

The total complex moment (G) which is the sum of $G_{\mbox{\scriptsize A}}$ and $G_{\mbox{\scriptsize B}}$ then becomes

$$G = i\gamma H_1 M_0 \left[\frac{\tau_A + \tau_B + \tau_A \tau_B (\alpha_A p_A + \alpha_B p_B)}{(1 + \alpha_A \tau_A) (1 + \alpha_B \tau_B) - 1} \right]$$
(15)

Since v is the component of G corresponding to the absorption line-shape function, the imaginary portion of G is observed as the in-phase component in the NMR experiment, which upon the assumption that $T_{2A} = T_{2B} = 0$ and $P_A = P_B$, gives

$$v = -\frac{1}{2} \gamma H_1 M_0 \left[\frac{\tau(\omega_A - \omega_B)^2}{\frac{1}{2} (\omega_A + \omega_B) - \omega} + \tau^2(\omega_A - \omega)^2(\omega_B - \omega)^2} \right]$$
(16)

which is the expression often used in the case of very narrow lines such as in proton NMR. In 23 Na NMR however, the lines are much broader than proton NMR and T_{2A} is usually not equal to T_{2B} . The equations for this case will be considered later.

In this study, we have used Fourier transform techniques in which the validity of the adaptation of this derivation (ie. the slow passage condition) is not completely obvious. Woessner (9) has verified its use by solving these equations in the Fourier transform case with equivalent results.

ALKALI METAL RATE STUDIES

In recent years, complexing agents have been synthesized which trap these labile metal cations to the extent that an exchange phenomenon may be observed. This has drawn interest from the biological community as well as from chemists since these complexing agents might be used as models in simulating the processes which govern ion-transport through membranes in biological systems.

Crown ethers, developed by Pederson (10) were the first such complexing agents to appear. A typical "crown" is shown in Figure 1.

Figure 1. Dibenzo-18-crown-6

Schori, Jagur-Grodzinski, Luz and Shporer (11) were the first investigators to utilize these crowns to do an actual 23 Na rate study, applying the modified Bloch equations to the 23 Na NMR experiment. They studied the effect of temperature on the linewidth of the single broad absorption which they observed with the solvent dimethylformamide. Because of the broadness of the lines they did not observe two separate peaks but were able to fit the line broadening of the single absorption to the modified Bloch equations. For the case of equal populations, ie, the concentration of free sodium equal to that of complexed sodium at $^{-13^{\circ}}$ C, Schori, et. al. reported a τ value of about $^{10^{-3}}$ seconds and an

activation energy of 12.5 Kcal.

Wong, Konizer and Smid studied these systems by using proton NMR with several ethereal solvents and pyridine. They observed two sets of protons, one corresponding to complexed crown and the other from uncomplexed crown which they analysed at the coalescence temperature, obtaining results consistant with those of Schori, et. al. (12).

At the height of the interest in crown ethers, Lehn (13) introduced a class of complexing agents (cryptands or simply crypts) which selectively complex metal cations to an even greater extent than do the crown ethers. Crypts are bicyclic molecules in which the length of the three ether strands may be changed in order to accommodate different cations. A typical crypt is shown in Figure 2.

$$N \longrightarrow 0 \longrightarrow 0 \longrightarrow N$$

Figure 2. 2-2-2 crypt used for the complexation of 23 Na.

Lehn and co-workers (13-15) studied the complexing ability of these molecules by utilizing proton as well as ^{13}C NMR in aqueous solution. They have tabulated rate constants and $\Delta\text{G}^{\ddagger}$ values for many metal cations at their coalescence temperatures. Of particular interest to this study is the rate constant of ^{23}Na in water which is 27 sec⁻¹ at 3° C with $\Delta\text{G}^{\ddagger}$ = 14.2 Kcal.

In 1973, the first example of an actual two line rate experiment with ²³Na NMR was published by Ceraso and Dye (16). They studied a solution of 0.6M NaBr and 0.3M crypt in ethylenediamine, observing two lines whose

linewidths were not equal. For this case, the modified Bloch equations become:

$$v = -\gamma H_1 M_0 \left[\frac{SU + TV}{S^2 + T^2} \right]$$
 (16)

where

$$S = \frac{\dot{P}_{A}}{T_{2A}} + \frac{\dot{P}_{B}}{T_{2B}} + \frac{\tau}{T_{2A}T_{2B}} - \tau(\omega_{A} - \omega) (\omega_{B} - \omega)$$
 (17)

$$U = 1 + \tau(p_A/T_{2A} + p_R/T_{2B})$$
 (18)

$$T = (p_A^{\omega}_A + p_B^{\omega}_B - \omega) + \tau \left[\frac{(\omega_A^{-\omega})}{T_{2B}} + \frac{(\omega_B^{-\omega})}{T_{2A}} \right]$$
 (19)

$$V = \tau (p_B \omega_A + p_A \omega_B - \omega)$$
 (20)

where $\boldsymbol{p}_{\boldsymbol{A}}$ is the population at site A and $\boldsymbol{\tau}$ is the lifetime of interaction defined by

$$\tau = \frac{\tau_A \tau_B}{\tau_A + \tau_B} \tag{21}$$

This experiment was unique in that the reaction times and chemical shifts could be measured in separate experiments. A total lineshape analysis was used, which employed a generalized weighted nonlinear least-squares program (20) to fit the data at several temperatures. A τ value of about 10^{-3} sec. at 40° C with ΔG^{\ddagger} = 14.8 Kcal at 50° C was obtained, agreeing with Lehn's results in aqueous solution.

CHAPTER III

EXPERIMENTAL

GLASSWARE CLEANING

All glassware used for the NMR studies was soaked in aqua regia for at least three hours and then rinsed in an HF cleaning solution. The glassware was then rinsed several times with distilled water and then with conductance water several more times and dried at 110° overnight.

SOLVENT PURIFICATION

All solvents were purified in the lab of Dr. Alexander Popov and the reader is directed to the thesis of Mark S. Greenberg for this information.

CHEMICAL PURIFICATION

All salts were reagent grade and no further purification was done except drying at 110° for at least ten hours. Salts were then stored in desiccators over CaSO₄.

SAMPLE PREPARATION

Salts and crypt were weighed directly into NMR tubes and then rough pumped for several hours in a vacuum desiccator. The NMR tubes were graduated, which allowed the solvent to be delivered directly into the tube in a dry box.

INSTRUMENTATION

<u>Super Con-</u> Many of the ²³Na chemical shift data were taken on a highly modified NMRS-MP-1000 spectrometer, operating at 60.06 MHz at a field of 53 kG. The time sharing method of Baker (17) was employed and the instrument utilized 5mm crossed coil probes. This system was interfaced to a Nicolet 1083 computer for time averaging capabilities.

<u>Varian DA-60-</u> The DA-60 utilizes an extremely homogeneous magnetic field at 15.87 MHz with a greatly modified NMRS-MP-1000 spectrometer in the pulse mode. The field is locked by a home-built lock probe (21) which uses the DA-60 console to lock on a proton resonance. The lock was very stable, drifting on an average of five Hz in twelve hours. Block diagrams for the DA-60 and the lock system are shown in Figures 3 and 4. The DA-60 is interfaced to a Nicolet 1083 computer for time averaging of spectra and also for on-line Fourier transformation of data.

DATA MANIPULATION

Data collected with the Nicolet 1083 computer were dumped onto paper-tape in octal via program PATPRT (18), then converted to decimal by using program CONVERT (19), and ordered in a form compatable with KINFIT (20). KINFIT, a generalized weighted non-linear least-squares program, was then used to fit the lineshape data to the modified Bloch equations.

A modification to the Nicolet 1074 version of FTNMR was also utilized to dump data as shown in the Appendix.

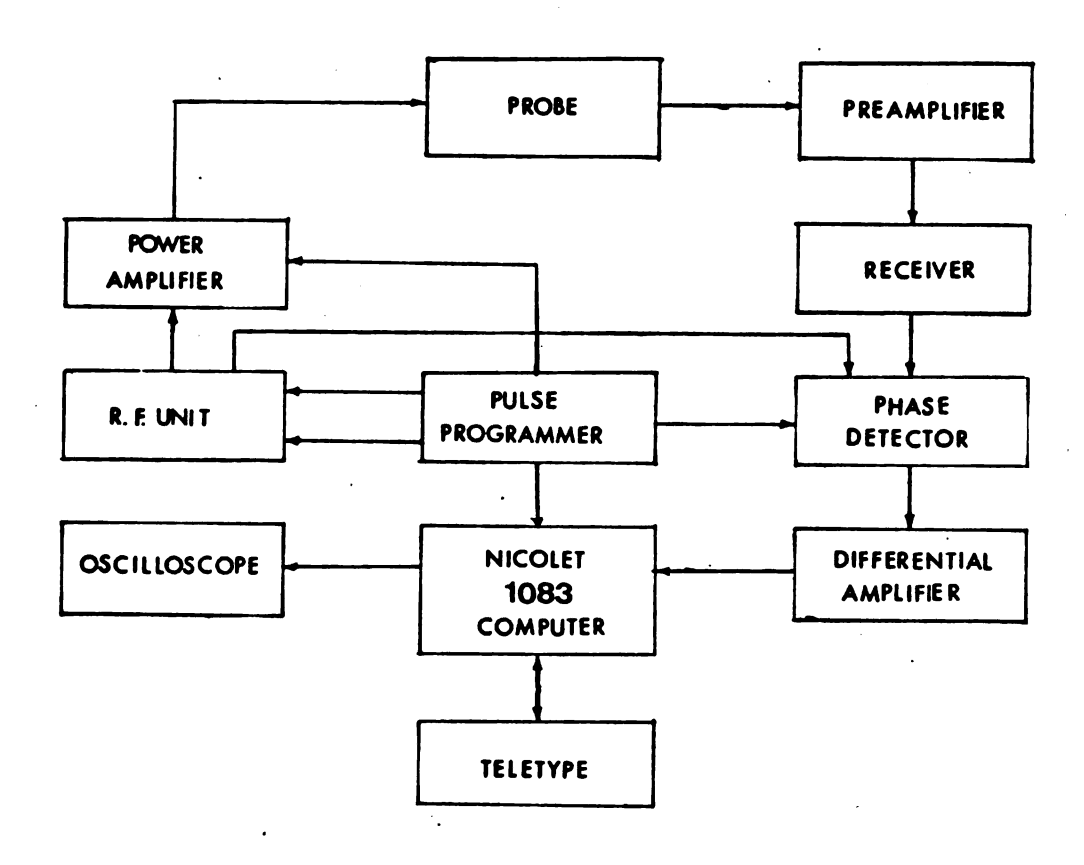


Figure 3. Block Diagram of the DA-60

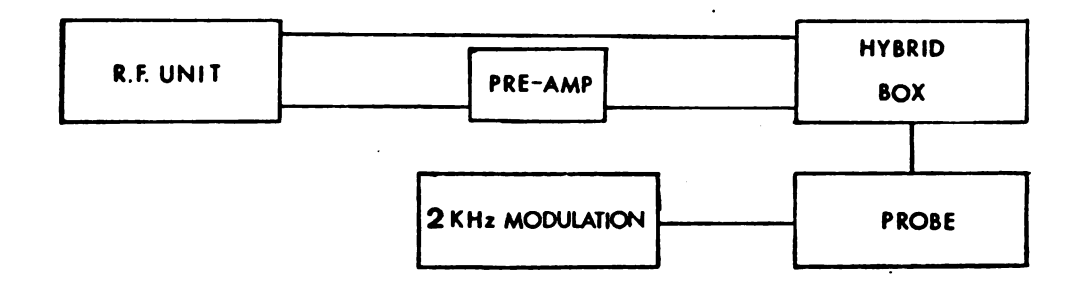


Figure 4. Block Diagram of the Lock System

CHAPTER IV

RESULTS

THE NON-EXCHANGING SYSTEM

The goal of this study was to determine the extent to which the crypt protects the complexed cation from neighboring species in solution. Figure 5. shows a diagram of the complexed cation. From the structure of the cryptate, one would expect very little interaction between the cation and the environment outside the crypt. A rather symmetric environment is provided for the cation by the crypt which, in the absence of distortion, would produce relatively narrow lines. We expected therefore, that the chemical shifts and linewidths of the complexed cation would be independent of the solvent. Table 1 shows the chemical shift of the complexed cation in several solvents.

In most cases, the chemical shift is relatively independent of solvent but there are four noticable exceptions to this rule; namely water, acetonitrile, acetone and ethylenediamine (EDA). One possible explanation for the behavior of these four solvents might reside in the fact that the geometry of the crypt provides small holes through which interaction with polar groups might take place. Water, acetone, acetonitrile and EDA all have small, polar residues whereas the other solvents (except methanol) have larger polar groups. The holes in the crypt might be more conducive to interactions with small molecules or polar groups than to large ones and could conceivably produce the observed behavior. Another possibility is that the cation might not be completely enclosed by the crypt in these solvents.

Naturally, this study was not without its problems, the most serious of which was solubility. Table 1 also lists those systems in which the solubility of the complex was not high enough to observe by using NMR. It is worth noting that crypt and the salt were soluble in these



Figure 5. Space Diagram of the Complexed ²³Na Cation.

solvents by themselves but together they precipitated from solution.

THE EXCHANGING CASE

In continuation of the results published by Ceraso and Dye (16), this work was designed to investigate the solvent dependence of the release of the sodium ion from the crypt. Four solvents were examined; tetrahydrofuran (THF), water, pyridine and EDA. The exchange had been studied in water previous to our work by utilizing proton NMR (13-15) so that a comparison of the results from proton and ²³Na NMR would be interesting. The study of several other systems was also attempted but was discontinued because the chemical shift was not large enough, or the two absorptions were too broad, thus producing only one broad peak. Sodium tetraphenylborate (NaTPB) in nitromethane and in propylene

Table 1. The Chemical Shift of 23 Na in Several Solvents

		СО	MPLEX		F	REE
Solvent	Salt	Conc.	$\Delta v_{1}^{\mathbf{a}}$	ΔPPM^{b}	$\Delta v_{1}^{\mathbf{a}}$	ΔPPM^{C}
PYRIDINE	NaTPB	0.2	40.	13.1	_	
DMF	NaTPB	0.2		13.4		5.2
PROPYLENE CARBONATE	NaTPB	0.2		13.2		9.2
THF	NaTPB	0.2	37	12.7	27	8.1
ACETONE	NaTPB	0.2		10.1		8.6
ACETONITRILE	NaTPB	0.2		9.5		8.0
METHANOL	NaI	0.2		11.9		9.5
WATER	NaTPB	0.2	60	9.2	11	0.9 ^b
EDA	NaBr	0.3	93	11.3	57	-13.0 ^b
DMSO	NaTPB	0.4		11.2		0.7
NITROMETHANE	NaTPB	0.4		11.5		15.6
WATER	NaC1					
WATER	NaTPB	,				
ETHYL AMINE	NaI					
ETHYL AMINE	NaTPB					
ETHYL AMINE	NaSCN					
METHANOL	NaTPB					
BENZENE	NaTPB					
ACETIC ACID	NaC104					
EDA	NaI					
THF	NaI					

a) Full-width at half-height

b) Referenced to 3M aqueous NaCl at 40°C

c) Referenced to saturated aqueous NaCl at 40°C

carbonate as well as NaI in acetonitrile yielded this type of behavior.

The systems ultimately used for rate studies were 0.4 M NaI and 0.2 M crypt in water, 0.6 M NaBr and 0.3 M crypt in EDA, 0.4 M NaTPB and 0.2 M crypt in pyridine and 0.4 M NaTPB and 0.2 M crypt in THF.

The modified Bloch equations appropriate to our system are

$$v = -\gamma H_1 M_0 \left[\frac{SU + TV}{S^2 + T^2} \right]$$
 (22)

where

$$S = \frac{P_A}{T_{2A}} + \frac{P_B}{T_{2B}} + \frac{T}{T_{2A}T_{2B}} - \tau(\omega - \omega)(\omega - \omega)$$
(23)

$$U = 1 + \tau(p_A/T_{2A} + p_B/T_{2B})$$
 (24)

$$T = (p_A^{\omega}_A + p_B^{\omega}_B - \omega) + \tau \left[\frac{(\omega_A - \omega)}{T_{2B}} + \frac{(\omega_B - \omega)}{T_{2A}} \right]$$
 (25)

$$V = \tau (p_B^{\omega} + p_A^{\omega} - \omega)$$
 (26)

where $\boldsymbol{p}_{\boldsymbol{A}}$ is the population at site A and $\boldsymbol{\tau}$ is the lifetime of interaction defined by

$$\tau = \frac{\tau_A \tau_B}{\tau_A + \tau_B} \tag{27}$$

 T_{2A} , T_{2B} , ω_A and ω_B were measured directly in separate experiments, and are tabulated in Tables 2 through 5; p_A and p_B were fixed by the initial concentration of salt and crypt so that τ and the amplitude were the only variables in our system.

These equations define the lineshape of a system at slow exchange to be two separate absorptions corresponding to nuclei in two separate

Table 2. The Variation of the Linewidth and Chemical Shift of the Complexed and Free 23 Na Cation with Temperature in EDA

Temp(°K)	$\frac{1}{T} \times 10^3 ($ °K $)$	$\Delta v_{\frac{1}{2}}^{a}(hz)$	T ₂ (msec)	ppm^b
		COMPLEXEDC		
293.4	3.409	90.1	3.534	11.1
299.8	3.336	76.7	4.151	11.4
305.5	3.274	67.5	4.714	11.6
308.3	3.244	61.1	5.208	11.5
314.6	3.179	53.7	5.976	11.6
321.5	3.111	47.0	6.773	11.9
325.6	3.072	43.4	7.332	11.8
332.2	3.011	38.1	8.347	11.9
340.9	2.934	33.5	9.508	11.9
		$\mathbf{f}_{REE}^{\mathbf{d}}$		
293.8	3.404	85.1	3.742	-13.10
299.5	3.340	73.9	4.306	-13.0
305.3	3.276	65.2	4.886	-12.9
311.2	3.214	59.0	5.400	-12.9
316.7	3.158	53.0	6.001	-12.9
322.3	3.103	48.3	6.593	-12.84
328.1	3.048	43.3	7.355	-12.8
333.2	3.002	40.0	7.956	-12.88
337.7	2.962	37.1	8.570	-12.71
343.3	2.913	34.0	9.370	-12.77

a) Full-width at half-height in Herz + 2 Herz, referenced to saturated NaCl of 11.9 Herz width.

b) Referenced to saturated aqueous NaCl + 3 Herz.

c) Concentration = 0.3 M crypt, 0.3 M NaBr.

d) Concentration = 0.6 M NaBr.

Table 3. The Variation of the Linewidth and Chemical Shift of the Complexed and Free 23 Na Cation with Temperature in THF

Temp(°K)	$\frac{1}{T} \times 10^3 ($ °K)	$\Delta v_{\frac{1}{2}}^{a}(hz)$	T ₂ (msec)	$\Delta \mathtt{PPM}^{\mathbf{b}}$
		COMPLEX	KEDC	
292.7	3.415	58.2	5.468	12.61
298.3	3.353	53.4	5.890	12.76
303.5	3.295	48.5	6.561	12.9
308.6	3.241	45.5	6.996	13.0
315.3	3.172	42.4	7.512	13.2
319.8	3.127	39.6	8.030	13.2
326.4	3.064	36.6	8.707	13.3
332.7	3.006	34.4	9.247	13.3
337.4	2.964	36.7	9.739	13.4
341.6	2.928	31.8	10.011	13.4
344.1	2.907	31.2	10.204	13.5
		FREE ^d		
298.9	3.346	35.3	9.007	8.1
303.9	3.291	34.5	9.226	8.2
308.6	3.241	33.8	9.428	8.3
316.0	3.165	32.7	9.737	8.4
321.1	3.115	32.3	9.849	8.5
326.3	3.065	31.8	10.011	8.6
332.9	3.004	31.3	10.179	2.9
338.0	2.959	31.1	10.245	2.9
343.3	2.913	30.9	10.317	3.0

a) Full-width at half-height in Herz ± 2 Herz, referenced to saturated aqueous NaCl of 12.3 hz width.

b) Referenced to saturated aqueous NaCl + 3 Herz.

c) Concentration = 0.2 M crypt, 0.2 M NaTPB.

d) Concentration = 0.4 M NaTPB.

Table 4. The Variation of the Linewidth and Chemical Shift of the Complexed and Free $^{23}\mathrm{Na}$ Cation with Temperature in Pyridine

Temp(°K)	$\frac{1}{T} \times 10^3 ($ °K $)$	$\Delta v_{\frac{1}{2}}^{a}(hz)$	T ₂ (msec)	$\Delta \mathtt{PPM}^{\mathbf{b}}$
	COMPLEXED C			
298.7	3.348	52.3	6.084	13.1
306.1	3.267	47.2	6.746	13.2
311.8	3.208	44.0	7.227	13.3
316.9	3.156	41.3	7.699	13.4
328.3	3.047	35.3	9.021	13.5
334.6	2.989	33.0	9.666	13.5
342.0	2.924	31.0	10.278	13.6
348.1	2.873	29.1	10.924	13.7
355.8	2.811	27.4	11.605	13.7
361.8	2.764	25.7	12.364	13.8
375.4	2.664	24.6	12.96	13.9
382.4	2.615	23.1	13.796	13.5
387.2	2.583	23.7	13.435	14.0
394.4	2.537	23.4	13.575	13.9
401.8	2.489	23.5	13.527	13.9
407.0	2.457	22.6	14.057	13.9
413.4	2.419	23.2	13.714	13.8
		FREE		
295.8	3.383	33.6	9.48	-0.3
318.2	3.145	28.3	11.23	0.3
330.8	3.025	25.2	12.38	0.6
342.2	2.924	24.1	13.19	0.7
353.5	2.830	23.1	13.78	0.9
361.5	2.768	23.6	13.48	1.1
374.0	2.675	23.1	13.79	1.3
385.6	2.595	23.0	13.84	1.4
398.6	2.510	23.1	13.79	1.7
407.0	2.458	24.7	12.91	2.1

Table 4 (continued)

413.5	2.420	24.1	13.19	2.3
418.0	2.393	24.7	12.91	2.3

- a) Full-width at half-height in Herz + 2 Herz, referenced to saturated aqueous NaCl of 12.3 hz width.
- b) Referenced to saturated aqueous NaCl + 3 Herz.
- c) Concentration = 0.2 M Crypt, 0.2 M NaTPB.
- d) Concentration = 0.4 M NaTPB.

Table 5. The Variation of the Linewidth and Chemical Shift of the Complexed and Free 23 Na Cation with Temperature in Water

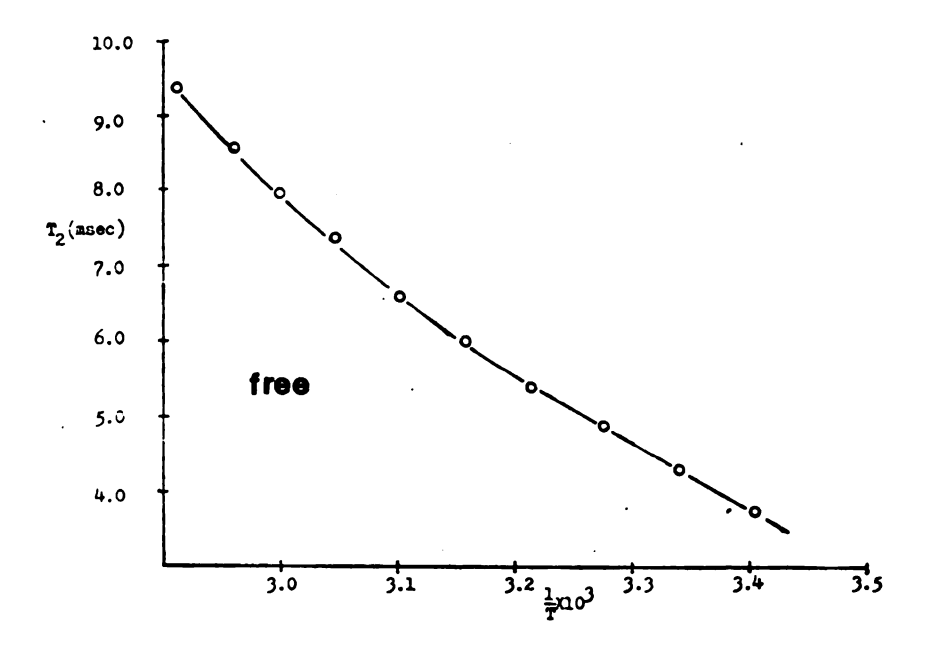
Temp(°K)	$\frac{1}{T} \times 10^3 ($ °K $)$	Δν <mark>i</mark> (hz)	T ₂ (msec)	$\Delta PPM^{\mathbf{b}}$
		COMPLEX	EDC	
276.0	3.624	170.6	1.866	8.2
281.5	3.553	144.3	2.206	8.4
286.6	3.490	117.9	2.699	8.6
292.4	3.421	103.9	3.063	8.8
294.2	3.400	94.7	3.361	9.2
298.2	3.354	83.0	3.836	9.2
302.9	3.302	79.0	4.027	9.2
308.5	3.242	63.5	5.013	9.6
313.8	3.187	57.2	5.564	9.8
319.1	3.134	52.4	6.079	10.0
323.9	3.088	47.6	6.692	10.2
327.8	3.051	43.8	7.268	10.2
334.0	2.995	40.0	7.956	10.4
339.3	2.948	36.8	8.643	10.6
		$\mathtt{FREE}^{ extbf{d}}$		
281.0	3.56	17.8	17.88	
287.1	3.49	14.9	21.36	0.9
294.4	3.40	13.8	23.07	0.9
306.5	3.26	11.8	26.98	
309.4	3.23	11.3	28.17	1.2
317.4	3.15	11.1	28.68	1.5
325.9	3.07	11.1	28.68	
330.5	3.03	11.1	28.68	1.5

a) Full-width at half-height in Herz + 2 Herz in the complexed case and 1 Herz in the free case, referenced to saturated aqueous NaCl of 12.8 hz.

b) Referenced to saturated aqueous NaCl + 3 hz.

c) Concentration = 0.2 M Crypt, 0.2 M NaI.

d) Concentration = 0.4 M NaI.



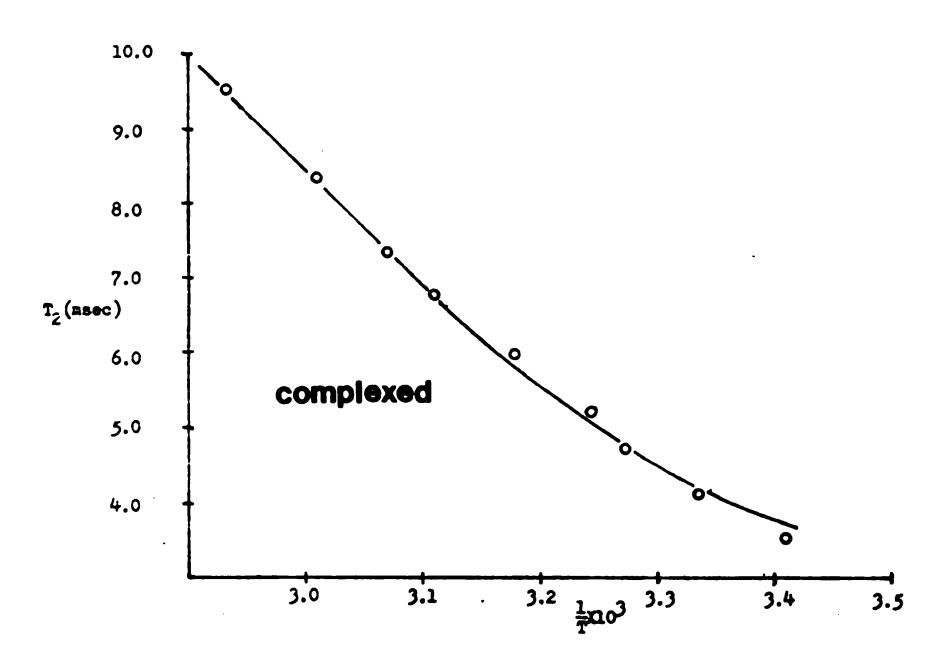
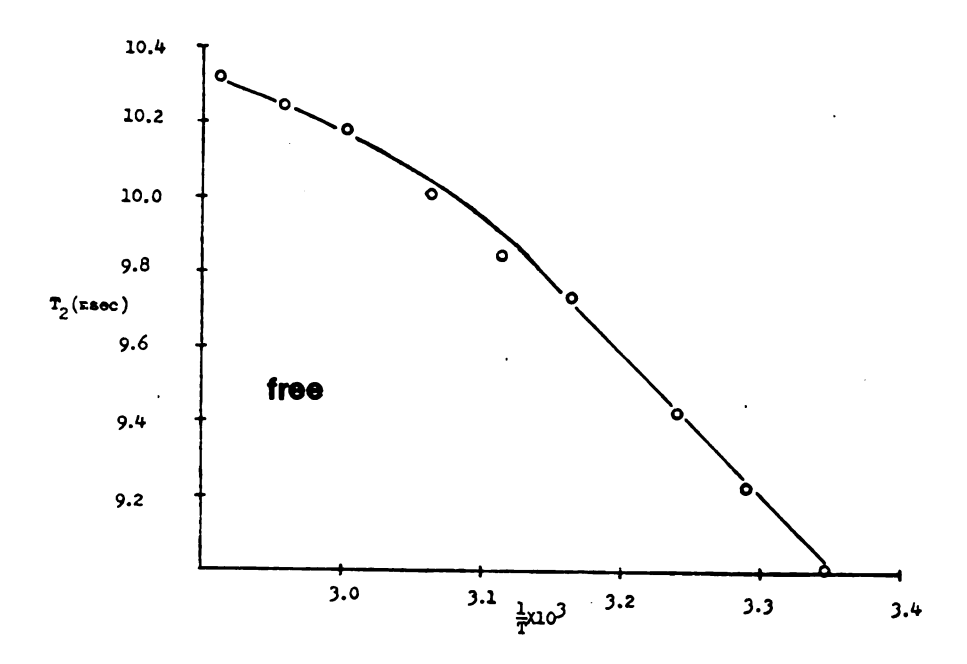


Figure 6. The Variation of T_2 with 1/T for EDA



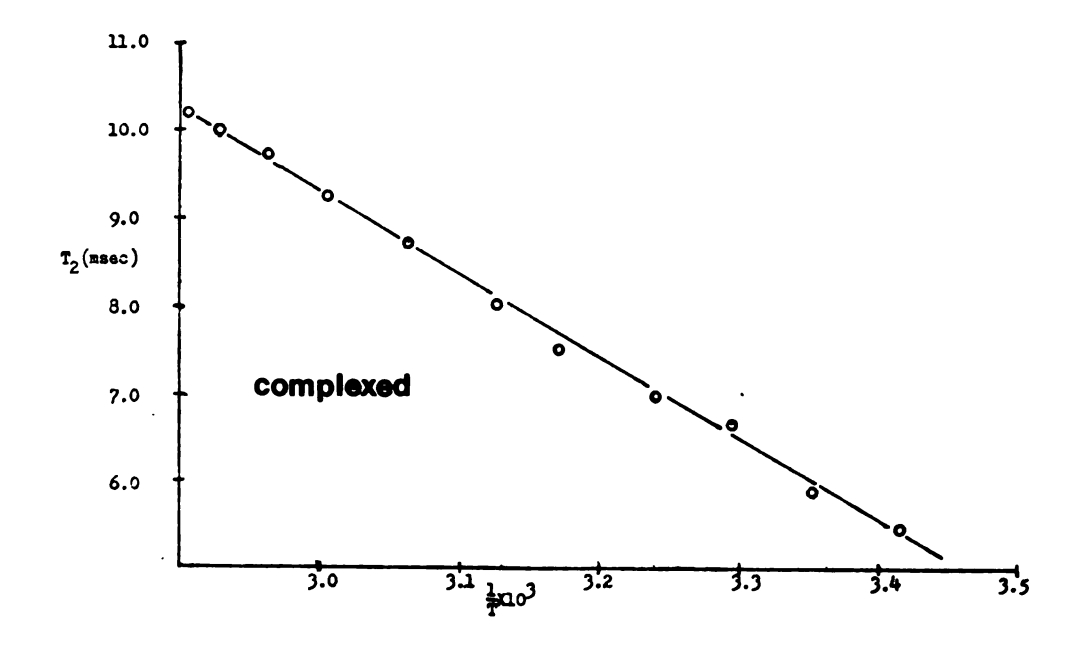


Figure 7. The Variation of T_2 with 1/T for THF

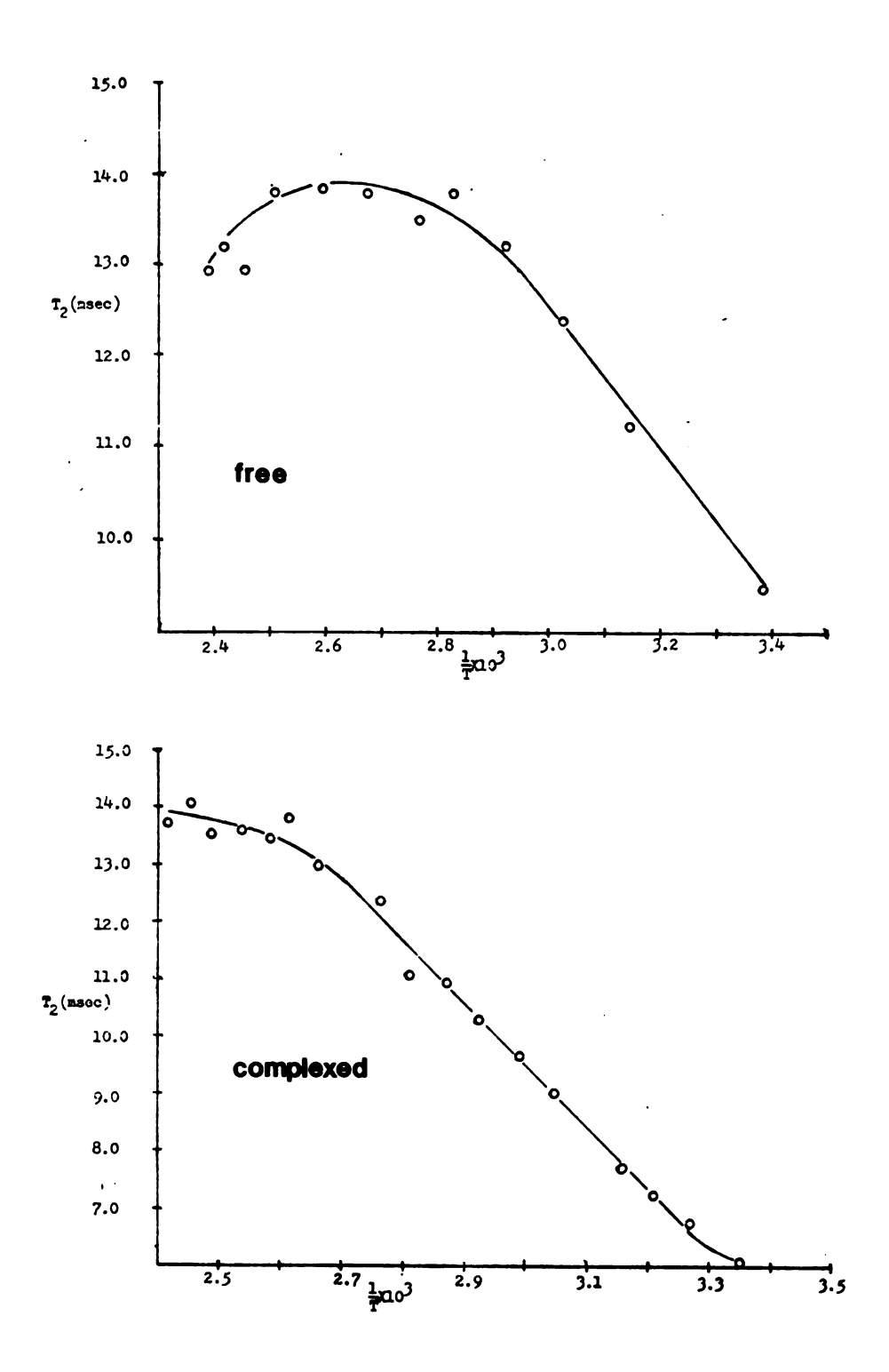
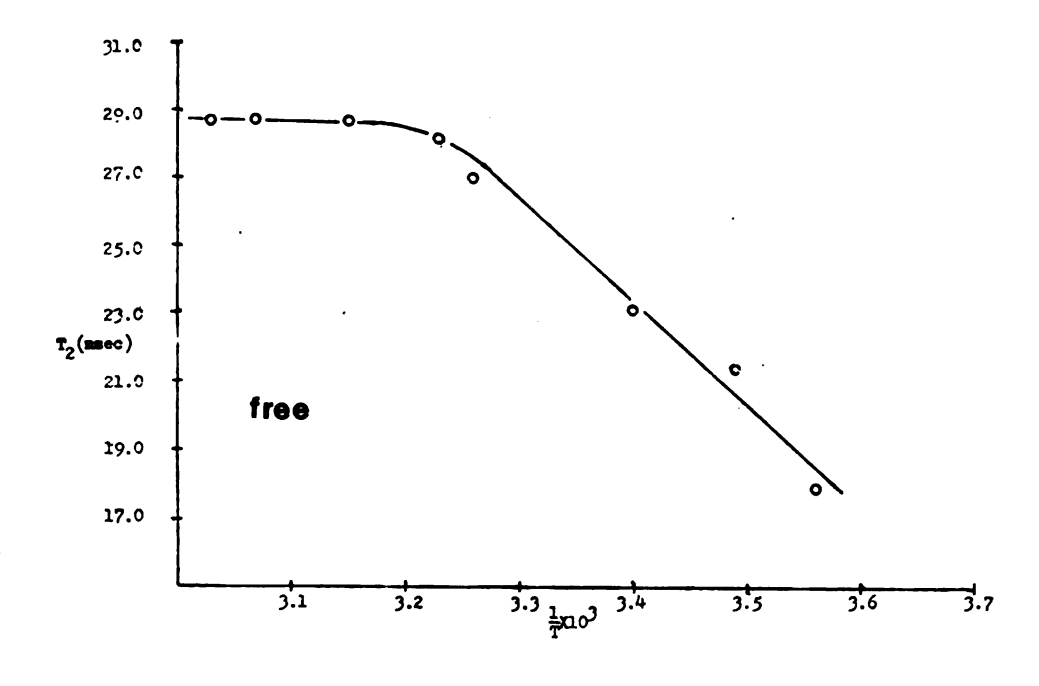


Figure 8. The Variation of T_2 with 1/T for Pyridine



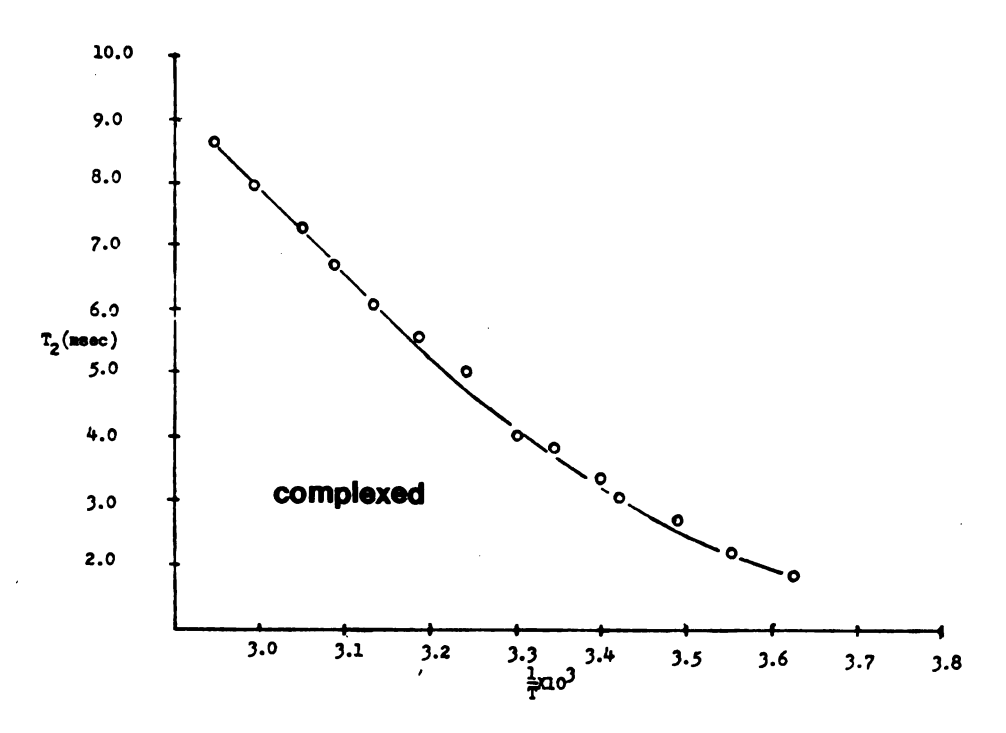


Figure 9. The Variation of T_2 with 1/T for Water

sites. As the exchange becomes more rapid, these lines broaden and begin to move together until, at more rapid exchange, they coalesce into one broad peak. If the rate of exchange is further increased, the broad absorption narrows considerably. This behavior is illustrated in Figures 10-13.

The lineshipes which are obtained in the four systems studied were fit to the modified Bloch equations by KINFIT in order to obtain τ . A five parameter fit was utilized in each case. These included a normalization constant, a baseline correction constant, a second order phase correction constant, a frequency correction constant, and τ . Figures 14-17 show typical computer fits of these lineshapes. X corresponds to the input data whereas 0 corresponds to the calculated value and = to those points in which the calculated value is equal to the input value within the resolution of the print-plot. The exchange in each solvent yielded very good results, with standard deviations in τ less than 5%. τ , τ_{2A} and τ_{2B} for each temperature are shown in Tables 6-9 and are displayed graphically in Figures 18-21. Table 10 shows the activation energies and $\Delta G^{o\frac{1}{2}}$ for the exchange in each solvent.

SUSCEPTIBILITY OF ETHYL AMINE

It has been reported by Live and Chan (24) that the magnetic susceptibility correction with an internal capillary reference to be made in a Varian FA-60 spectrometer is different from that in a

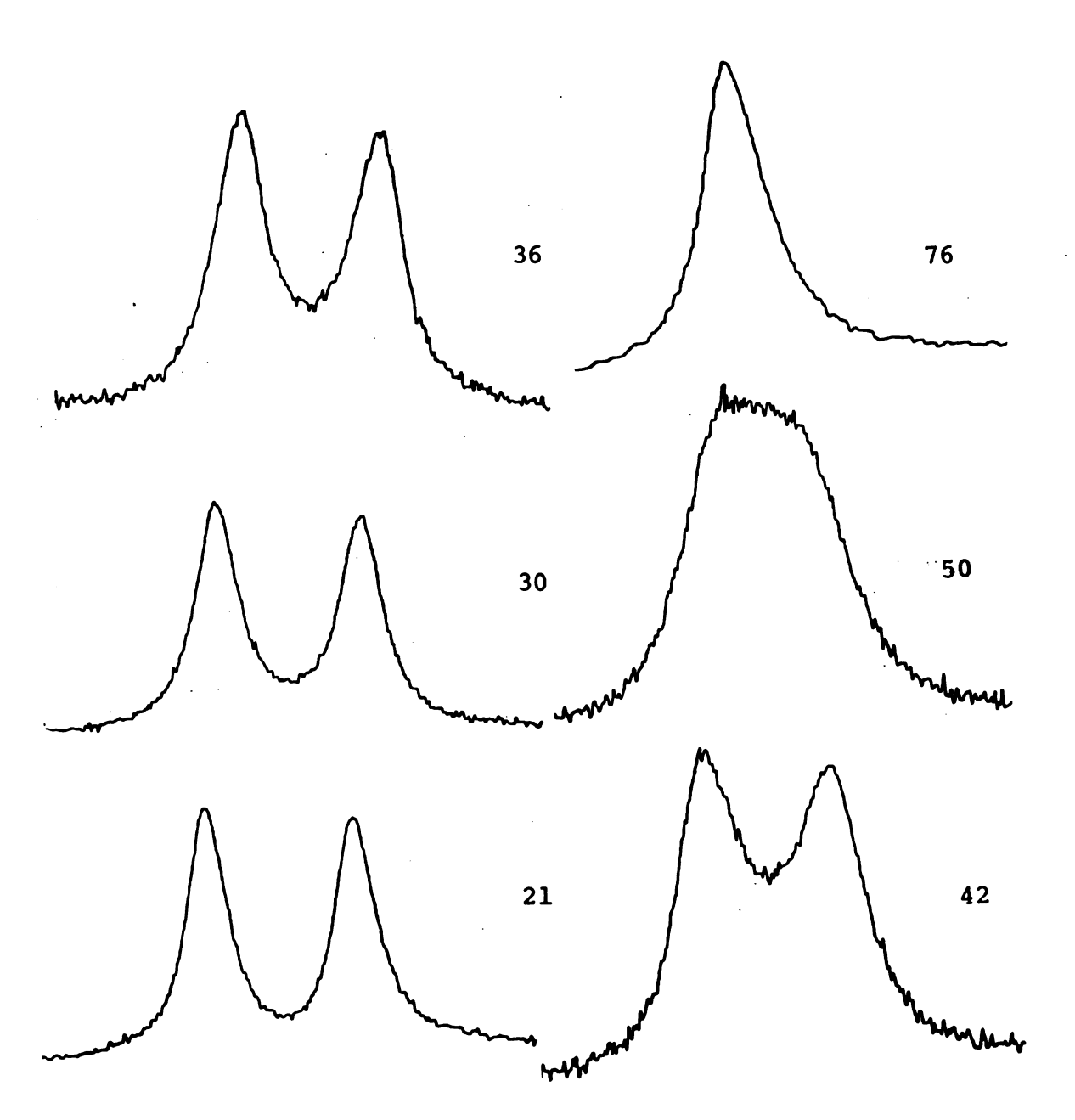


Figure 10. Typical Spectra Illustrating the Temperature Dependence of the NAR Lineshape for EDA

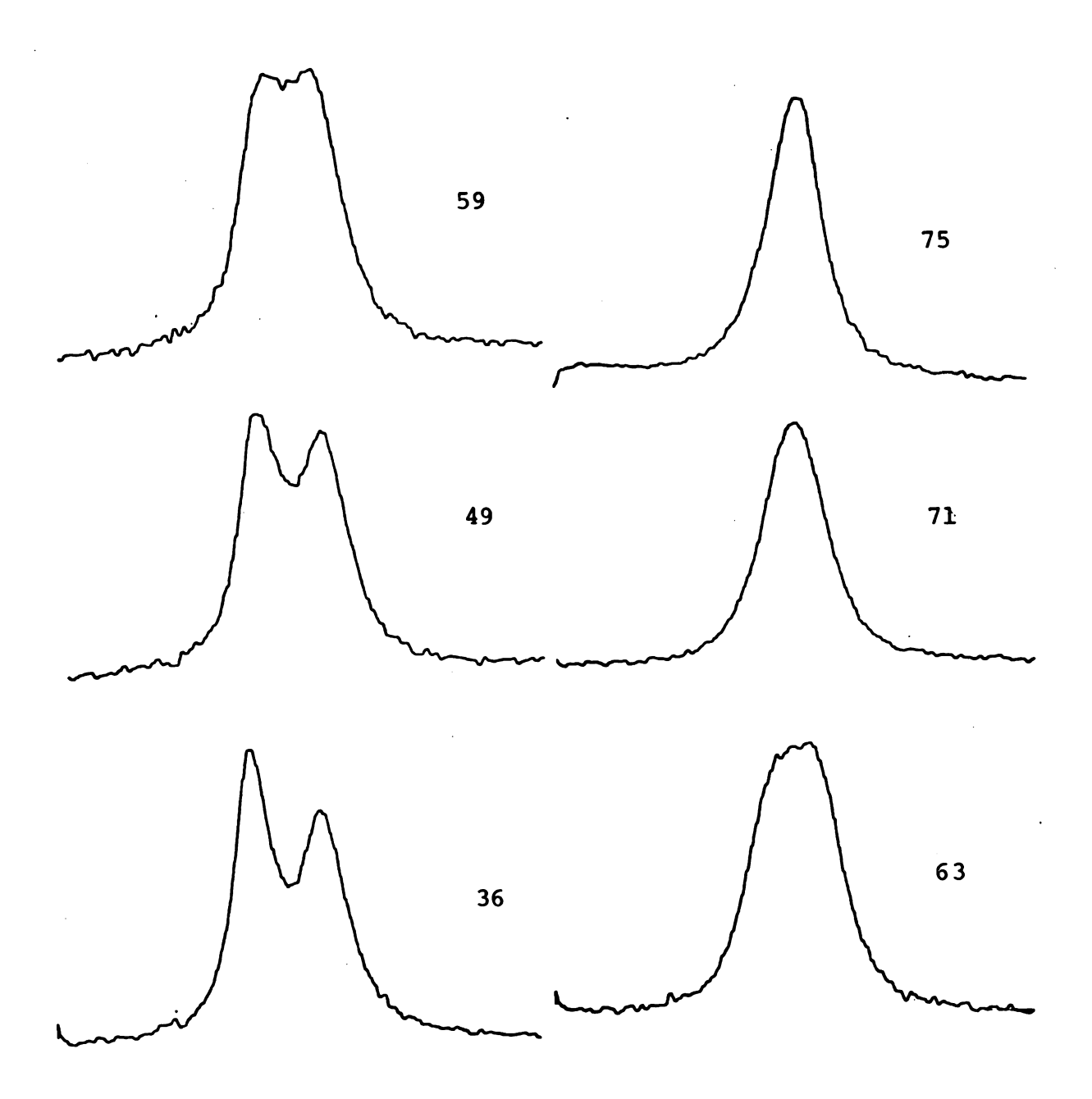


Figure 11. Typical Spectra Illustrating the Temperature Dependence of the Na NMR Lineshape for THF

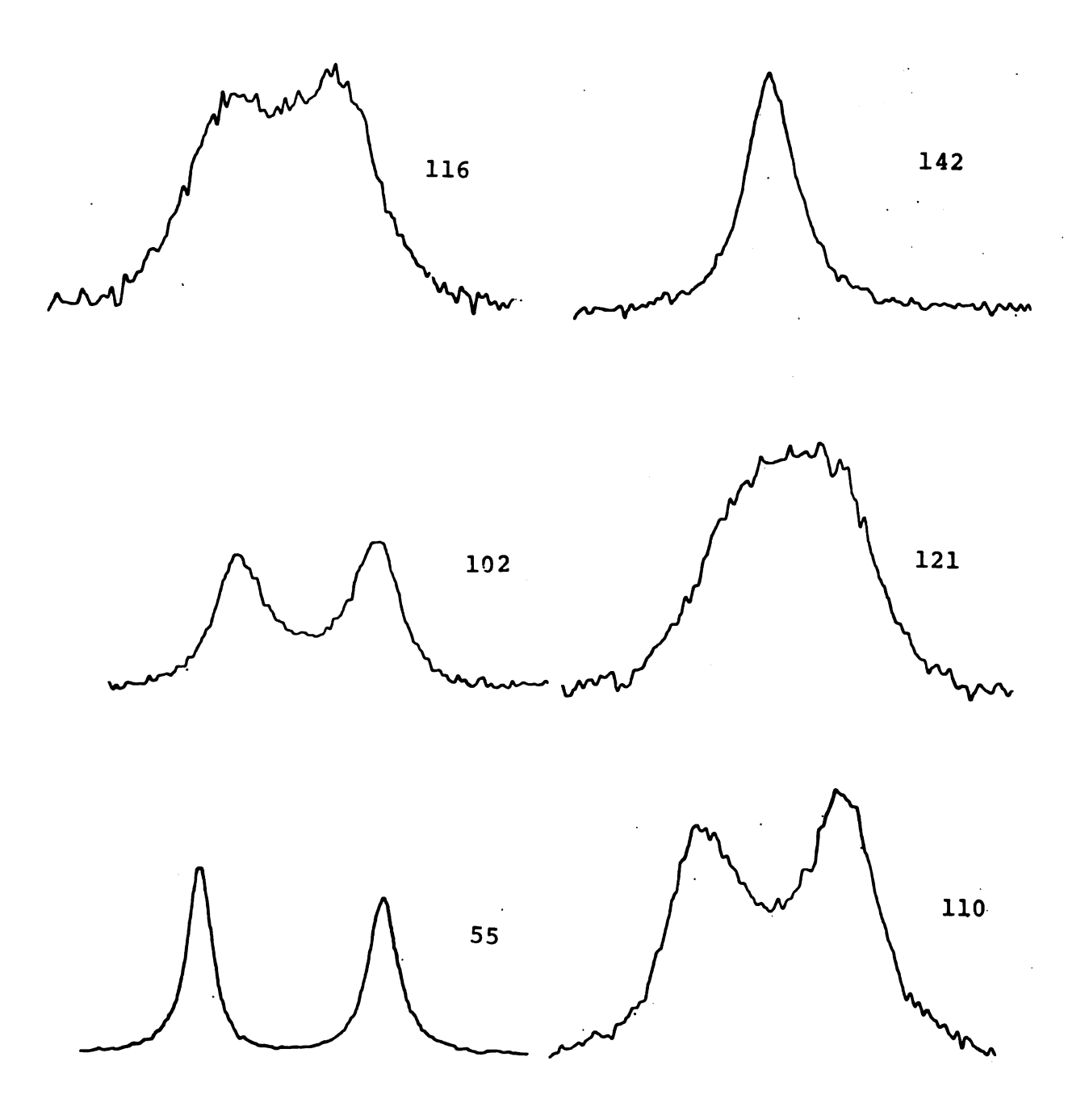


Figure 12. Typical Spectra Illustrating the Temperature Dependence of the 23Na NMR Lineshape for Pyridine

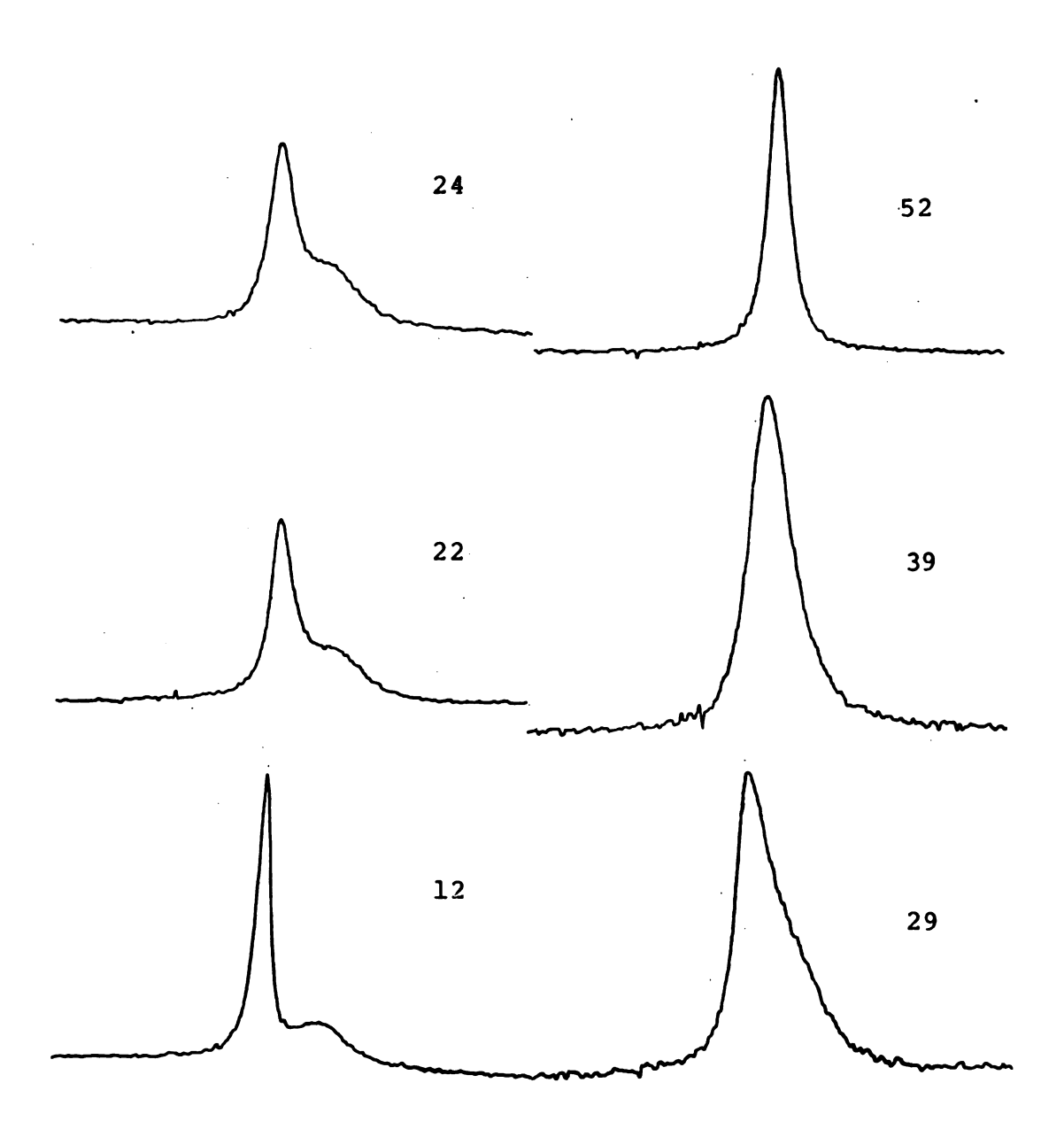


Figure 13. Typical Spectra Illustrating the Temperature Dependence of the ²³Na NMR Lineshape for Water

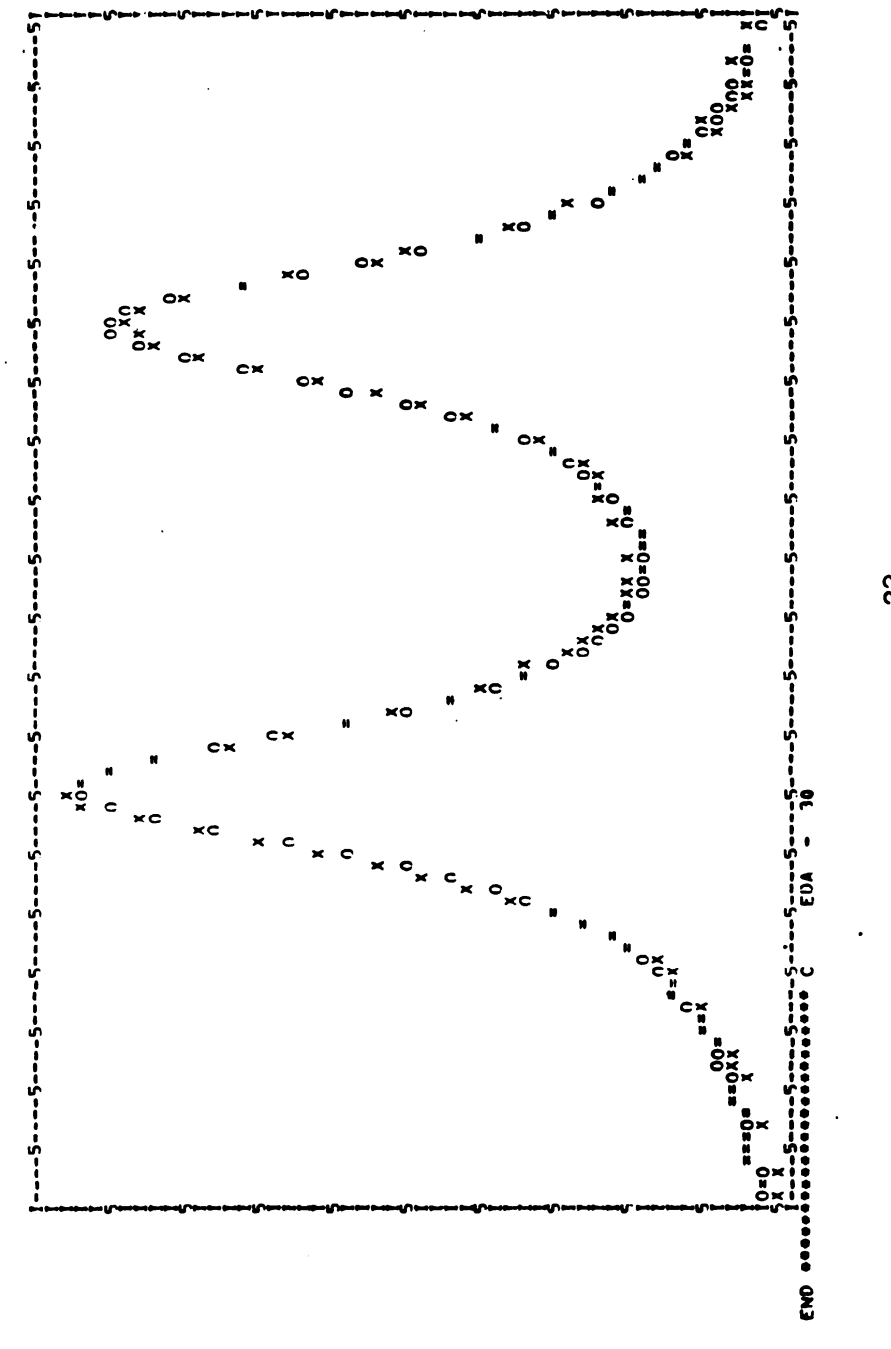
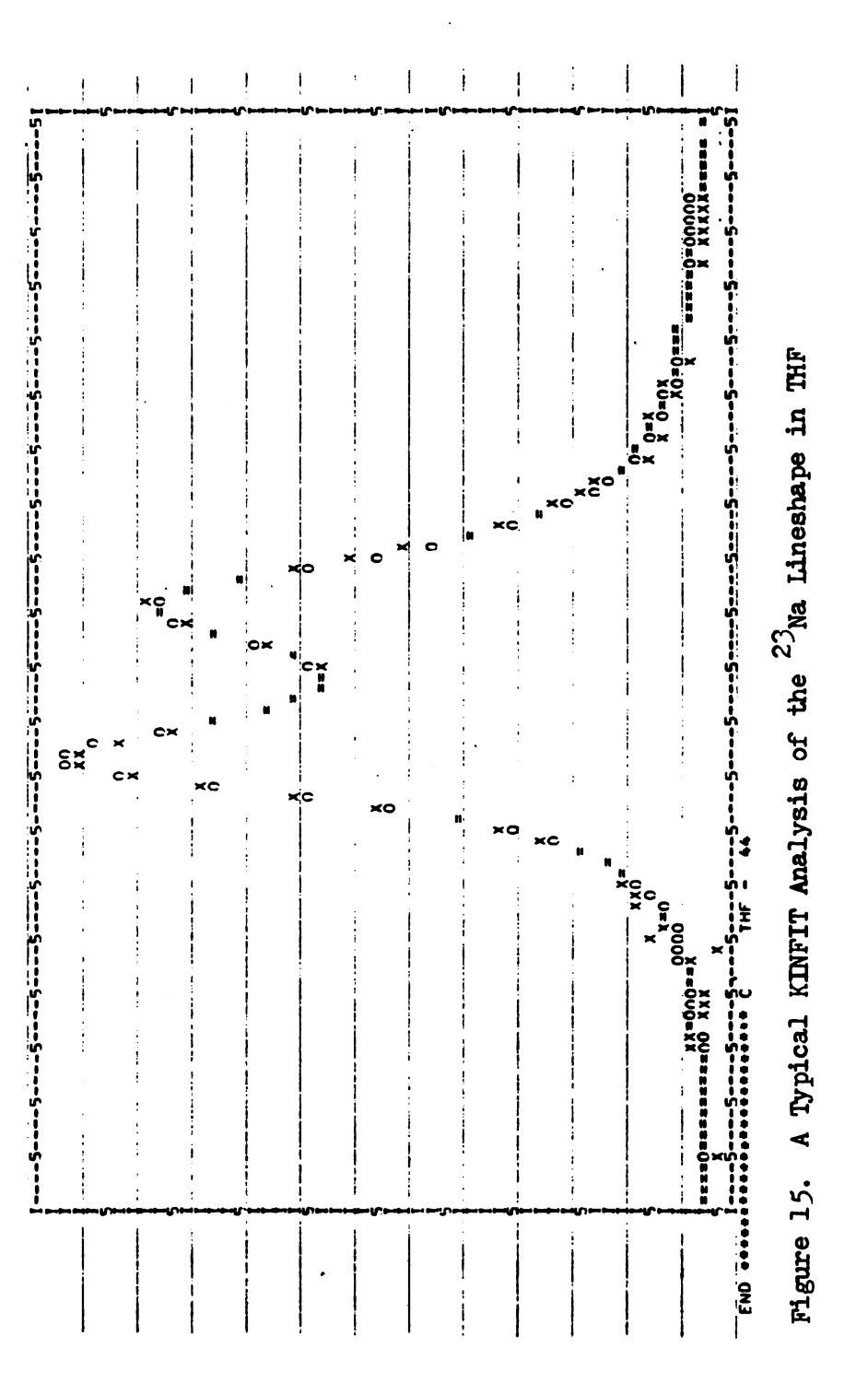
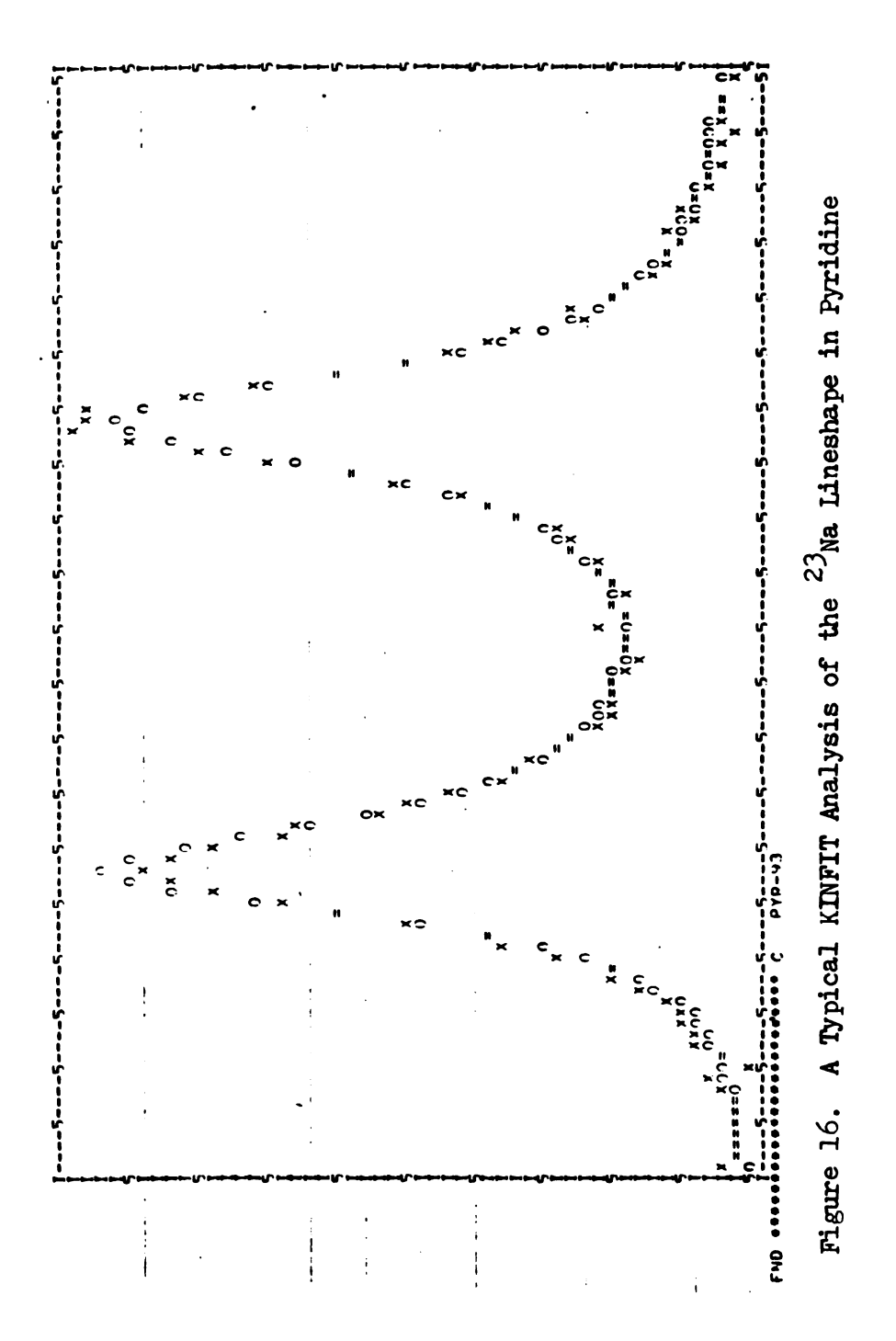


Figure 14. A Typical KINFIT Analysis of the $^{23}\mathrm{Na}$ Lineshape in EDA





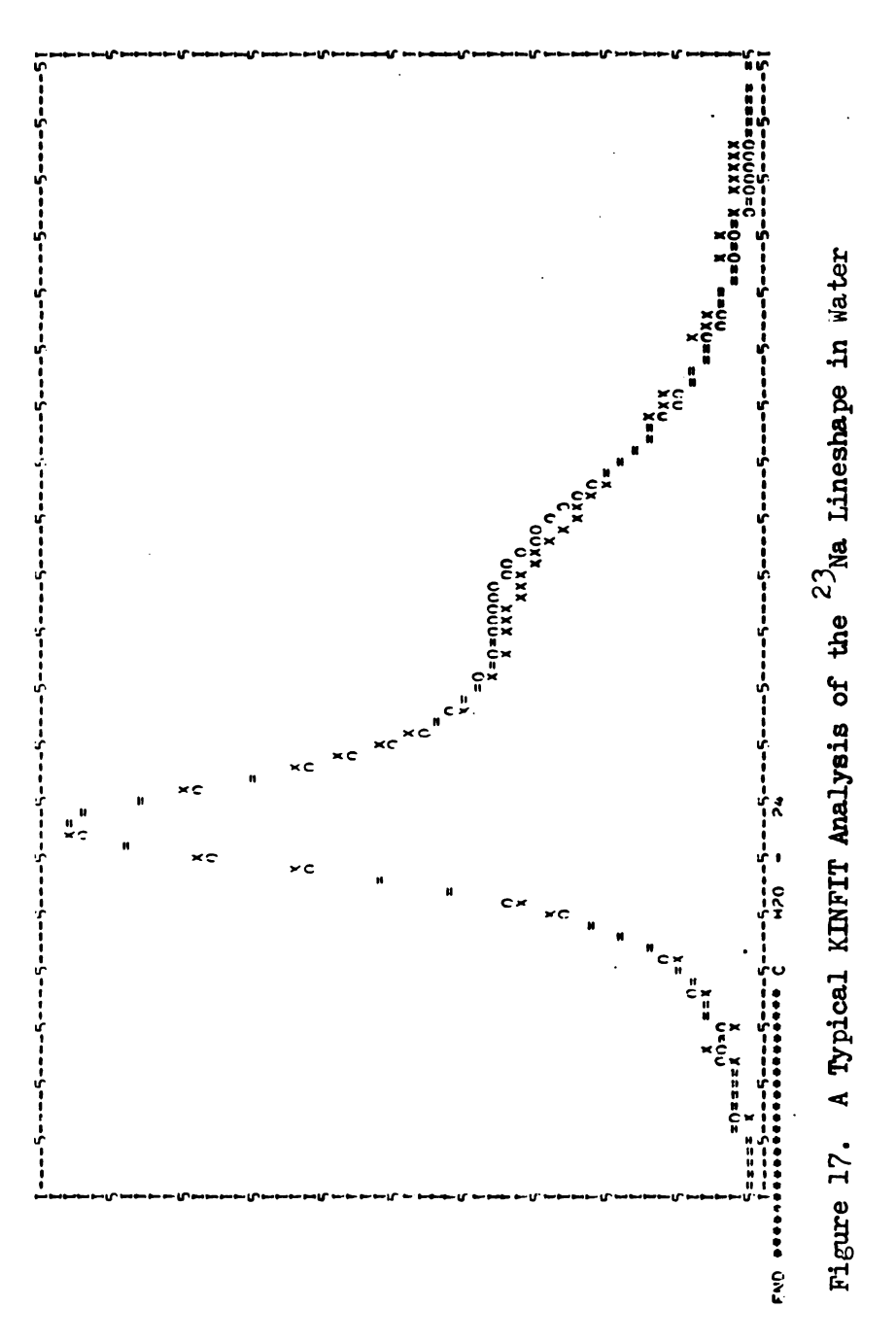


Table 6. The Temperature Dependence of the Exchange Time in EDA

T(°K)	$\frac{1}{T} \times 10^3$	τ(msec)	σ a	k	log k
288.7	3.464	4.81	0.176	103.9	4.64
294.5	3.396	4.01	0.104	124.6	4.83
303.6	3.294	2.338	0.033	213.9	5.366
309.4	3.233	1.603	2.016	311.9	5.742
311.2	3.214	1.413	0.013	354.0	5.869
314.6	3.179	1.126	0.008	444.0	6.096
315.6	3.169	1.048	0.008	477.0	6.168
318.2	3.143	0.0913	0.0076	561.0	6.330
323.4	3.093	0.6154	0.0045	812.4	6.700
327.0	3.059	0.4862	0.0035	1028.4	6.936
334.0	2.995	0.3111	0.0031	1607.2	7.382
342.2	2.923	0.1918	0.0016	2606.6	7.866
349.6	2.861	0.1238	0.0010	4040.1	8.304

a) Linear estimate of the standard deviation of τ .

Table 7. The Temperature Dependence of the Exchange Time in THF.

T(°K)	$1/T \times 10^3$	τ (msec)	а σ	k	log k
308.7	3.240	2.43	1.2	20.62	3.03
312.6	3.200	20.20	0.80	24.76	3.209
317.3	3.152	14.98	0.44	33.37	3.508
319.0	3.135	12.75	0.31	39.22	3.669
322.6	3.100	10.21	0.20	48.98	3.891
325.4	3.074	8.43	0.14	59.29	4.08
330.0	3.031	6.090	0.090	82.10	4.408
332.3	3.010	5.334	0.081	93.74	4.541
336.0	2.977	4.063	0.050	123.1	4.813
338.2	2.957	3.510	0.035	142.5	4.959
341.4	2.930	2.876	0.030	173.9	5.158
344.6	2.903	2.363	0.025	211.6	5.355
347.8	2.876	1.872	0.019	267.2	5.588

a) Linear estimate of the standard deviation of τ .

Table 8. The Temperature Dependence of the Exchange Time in Pyridine

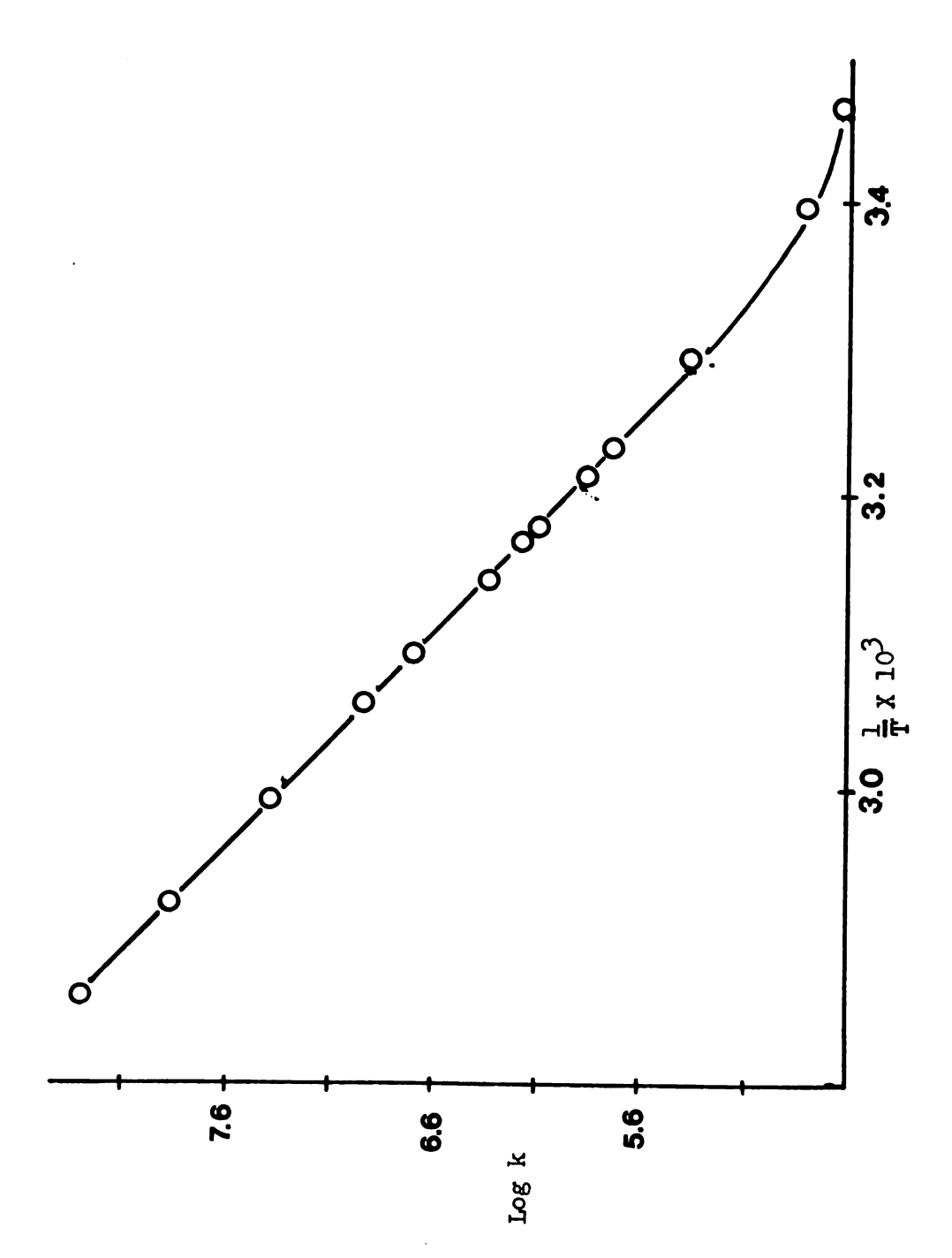
T(°K)	1/T × 10 ³	τ (msec)	a σ	k	log k
328.4	3.046	32	4.3	15	2.7
339.9	2.943	22	2.1	23	3.1
346.5	2.886	15	1.4	32	3.5
354.6	2.821	9.81	0.53	50.9	3.93
366.4	2.730	5.31	0.17	94.2	4.55
371.9	2.689	3.82	0.11	131	4.88
375.2	2.666	3.157	0.090	158.4	5.065
378.6	2.642	2.815	0.050	177.7	5.180
382.8	2.613	2.333	0.058	214.3	5.367
389.6	2.567	1.609	0.019	310.8	5.739
399.0	2.507	1.013	0.011	493.6	6.202
402.6	2.484	0.8607	0.0080	580.9	6.365
408.6	2.448	0.6611	0.0060	756.3	6.628
415.3	2.408	0.5051	0.0060	990.0	6.898

a) Linear estimate of the standard deviation of τ .

Table 9. The Temperature Dependence of the Exchange Time in Water

T	1/T × 10 ³	τ (msec)	a σ	1/2 τ	log k
276.2	3.621	35	3.1	14	2.7
285.2	3.507	11.34	0.46	44.10	3.786
295.4	3.386	4.335	0.067	115.3	4.748
296.8	3.370	3.875	0.050	129.0	4.860
300.0	3.333	2.877	0.040	173.8	5.158
302.4	3.307	2.178	0.023	229.6	5.436
303.7	3.292	2.030	0.022	246.3	5.507
306.9	3.258	1.616	0.020	307.4	5.728
310.2	3.224	1.120	0.020	415.0	6.031
312.5	3.201	0.8918	0.013	566.7	6.340
319.1	3.134	0.5122	0.0090	976.2	6.884
325.4	3.073	0.3333	0.0080	1500	7.313

a) Linear estimate of the standard deviation of τ .



The Variation of the Log of k with the Inverse of the Temperature in $\overline{\mathtt{EDA}}$ Figure 18.

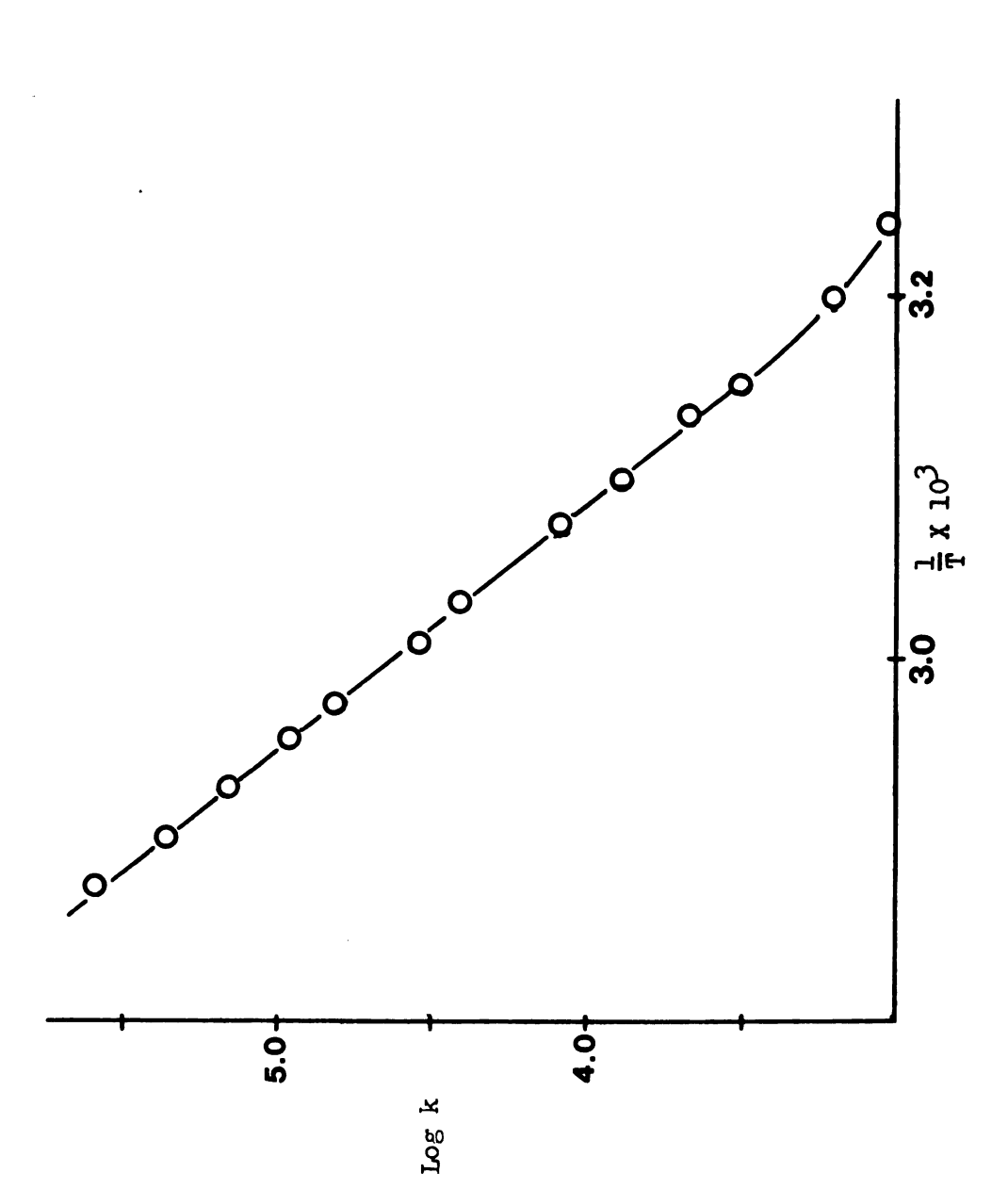


Figure 19. The Variation of the Log of k with the Inverse of the Temperature inTHF

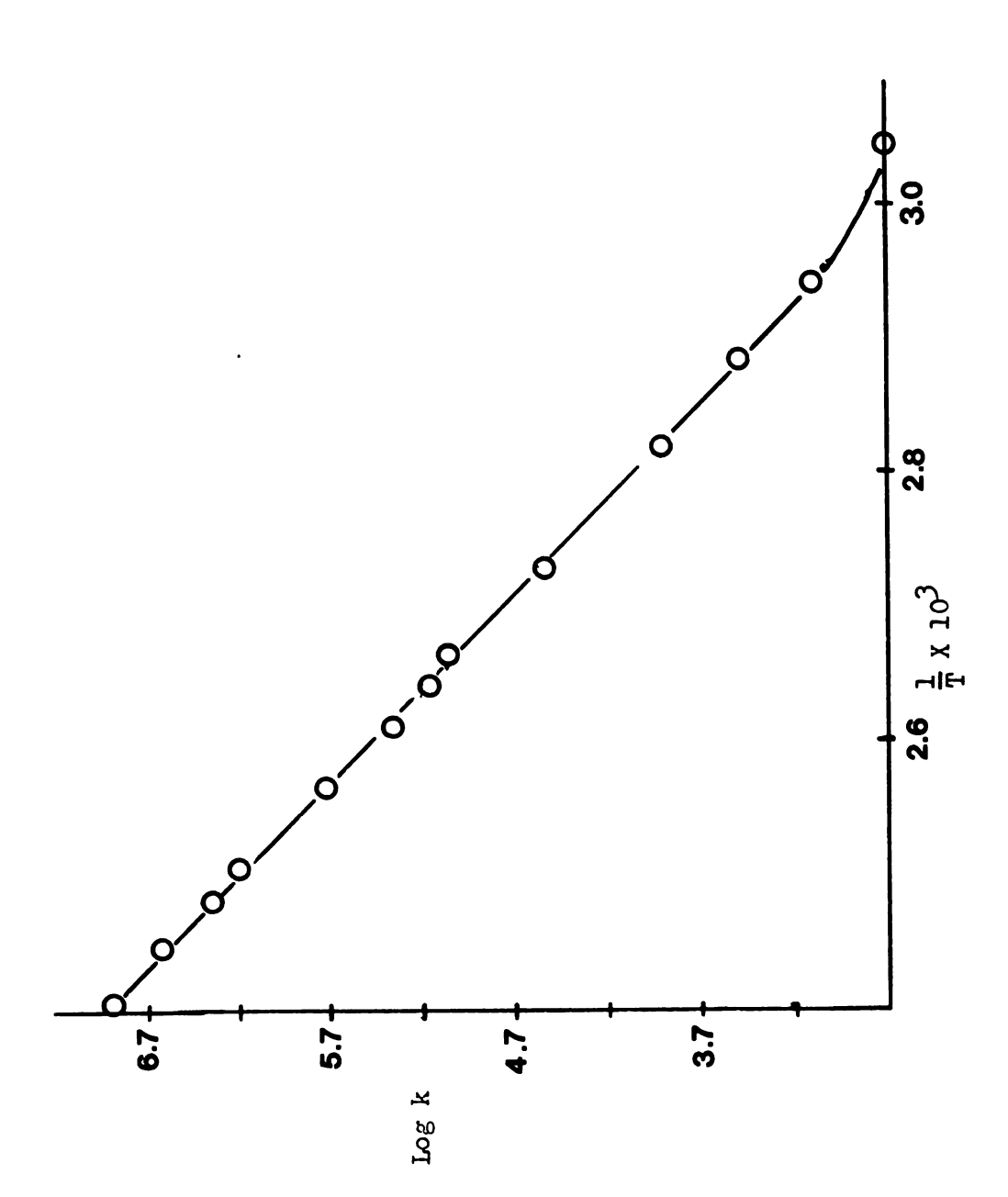
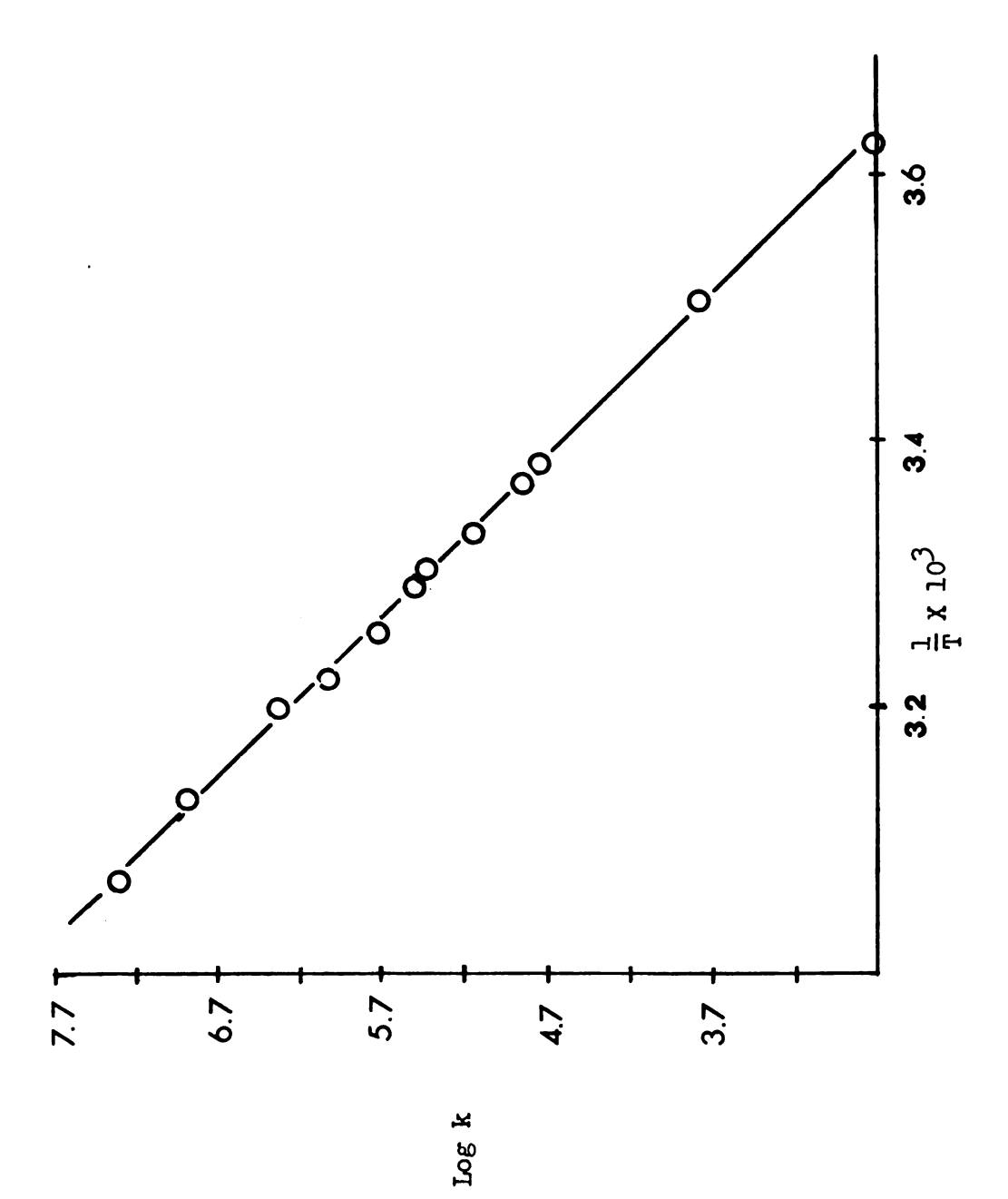


Figure 20. The Variation of the Log of k with the Inverse of the Temperature in Pyridine



The Variation of the Log of k with the Inverse of the Temperature in Water Figure 21.

superconducting HR-220 because of the different field geometries.

The equations are

$$\delta_{\text{corr}} = \delta_{\text{obs}} + \frac{2\pi}{3} (\chi_{\text{v}}^{\text{ref}} - \chi_{\text{v}}) \qquad (DA-60)$$
 (28)

$$\delta_{corr} = \delta_{obs} - \frac{4\pi}{3} (\chi_{v}^{ref} - \chi_{v}) \qquad (HR-220) \qquad (29)$$

Since spectrometers with both of these geometries were readily available to us, we presumed that by running an internally referenced sample in the two instruments, we could directly obtain the magnetic susceptibility of that sample. Solving these equations for χ_{ν}^{ref} we have

$$\chi_{v}^{\text{ref}} = \chi_{v} + \frac{1}{2\pi} \left(\delta_{\text{obs}}^{\text{DA-60}} - \delta_{\text{obs}}^{\text{HR-220}} \right)$$
 (30)

THF, internally referenced with a saturated aqueous NaCl solution was run first as a check on the method and yielded a value of -0.557 which is only a four percent difference from -0.577, the literature value (23). Next a .3 M NaTPB solution in THF was internally referenced by a saturated NaI solution in ethyl amine. Since the magnetic susceptibility of THF is known,

$$\chi_{V}^{\text{ref}} = 0.577 + \frac{1}{2\pi} \left[\frac{385.5}{15.87} - \frac{1437.}{60.06} \right] = -0.634$$
 (31)

This method of determining magnetic susceptibilities has one big advantage over the usual Gouy balance method; namely, the ease of the experiment. The entire undertaking can easily be completed in one afternoon.

Table 10. The Solvent Dependence of the Thermodynamic Parameters

Solvent	EA (Kca.	$A_{A}(\texttt{Kcal/mole})^{a}$	∆G ^{o≠} (Kcal/mole)	1/mole)	ΔH ^{o≠} (Kc	H ^{o≠} (Kcal/mole)	√S ^{o≠} (eu)	Î
Pyridine	14.19	(0.20) ^b	17.374	(0.004)	13.60	(0.20)	-12.66	(0.0)
EDA	12.99	(0.31)	13.574	(0.020)	12.40	(0.31)	-3.95	(0.0)
THF	14.39	(0.19)	16,219	(0.020)	13.80	(0.20)	-8.12	(0.6)
Water	16.67	(0.23)	14.493	(0.010)	16.08	(0.23)	5.30	(0.8)

a) The thermodynamic parameters were calculated for $298.2^{\rm O}{\rm K}$. b) Linear estimate of the standard deviation.

CONCLUSIONS

CHAPTER V

In this study we have utilized extremely powerful methods of data acquisition and analysis in order to precisely define these systems. As previously mentioned, T_2 and ω were measured in separate experiments, so the rate constants could be reliably determined. We also used a complete lineshape analysis, fitting the spectra at many temperatures to the appropriately modified Bloch equations, which was a procedure heretofore rarely utilized in NMR rate analyses. This has also been one of the first rate studies ever attempted in which T_{2A} and T_{2B} were appreciably different and since these parameters were so well defined, they provide a rigorous test of the applicability of the Bloch formulation to these systems.

There are several sources of error which could become important in this study since they could lead to serious distortion of the NMR line-shape. These include filtering, pulse feedthrough, saturation, delay time distortions and second order phase correction. Most of the above may be minimized instrumentally or else made provision for in computer fitting of data. Delay time distortion is the only variable which causes lineshape distortion which is not easily compensated for.

The delay time is the time between the rf pulse and the beginning of data acquisition. This is dead time which allows the receiver circuitry to recover from the large rf pulse and causes distortions in the following way. If two resonances in a spectrum are of very different T₂, then the faster relaxing nucleus would be attenuated to a much greater extent than the more slowly relaxing nucleus by the delay time and thereby "saturated" to a higher degree than the other. For example, the exchange in water involves a very broad (~100 hz) complexed sodium

resonance and a narrow (10 hz) free sodium resonance. The error in this case due to delay time distortions is less than 5% for a typical delay of 100μ sec, and can be corrected with P_A and P_B adjustments. In general, these distortions cause little trouble and the data very closely fit the lineshapes predicted by the modified Bloch equations with standard deviations in the computer fitting of less than 5%.

The rate constants which are reported in Tables 6-9 are defined by the following equations:

$$Na^+ + C_{222} \xrightarrow{k_1} NaC_{222}^+$$

 τ_A , the mean lifetime of the sodium ion resident in the cryptand, is related to the rate constant for the release of the cation, k_2 , by the following expression:

$$\frac{1}{\tau_A} = \frac{\text{rate of removal of sodium ion from cryptand by exchange}}{\text{the number of complexed sodium ions}}$$

$$= \frac{k_2 \text{ [NaC}^+]}{\text{[NaC}^+]} = k_2$$

$$\frac{1}{\tau_B} = \frac{k_1 [Na^+] [C]}{[Na^+]} = k_1 [C]$$

The values are reported as k_2 , the rate constant for the decomplexation.

No trend was observed between either donor number or dielectric constant of the solvent and the thermodynamic data reported in Table 10.

Cahen, Dye and Popov (25) reported a rough correlation between donor number and the activation energy of exchange for lithium cryptates, but

this correlation is not observed with sodium. The positive entropy of activation in the water case indicates participation of the solvent in the activated complex. This may be explained by the fact that water has a very high dielectric constant and interacts much more strongly with the sodium ion than the large organic complexed ion. The transition state seems to be composed of the partially solvated, partially complexed ion.

Several areas of this study pose interesting problems for further research. Of most interest would be the determination of the formation constants of sodium with C_{222} in these and other solvents. Calorimetry would be useful in determining heats of formation. Since the formation constants are known in six non-aqueous solvents for cesium salts (26), it has been suggested by Professor Dye that a competitive complexation for the C_{222} between sodium ion and cesium ion be undertaken. This "bootstrap" approach could be undertaken using a variety of ligands and metal cations to competitively complex sodium ion and C_{222} in order to determine this formation constant.

Another interesting problem for study is presented by the non-exchanging system in pyridine. In this solvent, the plot of T₂ with the inverse of temperature showed a curved behavior which could not be explained by normal viscosity effects. Since this effect was observed in both the free and complexed case, ion-pairing and direct solvent effects would seem to be ruled out. Perhaps a concentration dependence of this phenomenon would provide insight into its origin.

Finally, a competitive study using two different cations of similar

formation constant with a cryptand would be very interesting since the NMR facility at Michigan State University is fully multinuclear. The exchange phenomenon of both nuclei could be documented easily and utilized as a yet more rigorous test of the Bloch formulation. Formation constants and other properties of these cryptands will become increasingly important as both the chemical industry and the academic community discover the complexing ability and selectivity of these cryptands and as they begin to utilize them in areas such as ion chromatography, specific ion leachers, etc.

LITERATURE CITED

CHAPTER VI

LITERATURE CITED

- (1) C. Deverell and R. E. Richards, Mol. Phys., 10, 551 (1966).
- (2) R. Erlich and A. I. Popov, J. Amer. Chem. Soc., 93, 5620 (1971).
- (3) M. Herlem and A. I. Popov, J. Amer. Chem. Soc., 94, 1431 (1972).
- (4) E. G. Bloor and R. G. Kidd, Can. J. Chem., 46, 3425 (1968).
- (5) E. G. Bloor and R. G. Kidd, Can. J. Chem., 50, 3926 (1972).
- (6) R. Erlich, M. S. Greenberg and A. I. Popov, <u>Spectrochimica Acta</u>, 29A, 543 (1973).
- (7) M. S. Greenberg, R. L. Bodner and A. I. Popov, <u>J. Phys. Chem.</u>, 77, 2449 (1973).
- (8) J. A. Pople, W. G. Schneider and H. J. Bernstein, "High Resolution Nuclear Magnetic Resonance", McGraw-Hill, p. 218, 1959.
- (9) D. E. Woessner, J. Chem. Phys., 35, 41 (1961).
- (10) C. J. Pederson, J. Amer. Chem. Soc., 86, 7017 (1967).
- (11) E. Schori, J. Jagur-Grodzinski, Z. Luz and M. Shporer, <u>J. Amer.</u> Chem. Soc., 93, 7133 (1971).
- (12) K. H. Wong, G. Konizer and J. Smid, <u>J. Amer. Chem. Soc.</u>, 92, 666 (1970).
- (13) B. Dietrich, J. M. Lehn and J. P. Sauvage, <u>Tetrahedron Letters</u>, 2885 and 2889 (1969).
- (14) J. M. Lehn, J. P. Sauvage, B. Dietrich, <u>J. Amer. Chem. Soc.</u>, 92, 2916 (1970).
- (15) B. Dietrich, J. M. Lehn, J. P. Sauvage, <u>J. C. S. Chem. Comm.</u>, 15 (1973).
- (16) J. M. Ceraso and J. L. Dye, J. Amer. Chem. Soc., 95, 4432 (1973).
- (17) E. B. Baker, L. W. Burd and G. N. Root, <u>Rev. Sci. Inst.</u>, 36, 1495 (1965)
- (18) See Appendix.
- (19) See Appendix.

- (20) V. A. Nicely and J. L. Dye, J. Chem. Ed., 48, 443 (1971).
- (21) The lock probe was designed and built by Dr. David Wright and Dr. Joseph Ceraso.
- (22) M. S. Greenberg, Ph.D. Thesis, Michigan State University, East Lansing, Michigan, 1974.
- (23) J. M. Ceraso and J. L. Dye, J. Chem. Phys., 61, 1585, (1974).
- (24) D. H. Live and S. I. Chan, Anal. Chem., 42, 791 (1970).
- (25) Y. M. Cahen, J. L. Dye and A. I. Popov, <u>J. Chem. Phys.</u>, 79, 1292 (1975).
- (26) E. Mei, Ph.D Thesis, Michigan State University, East Lansing, Michigan, 1977.

APPENDIX

CHAPTER VII

DESCRIPTION OF THE MODIFICATION TO THE NICOLET 1074 VERSION OF FTNMR IN ORDER TO DUMP DATA

The Nicolet 1074 version of FTNMR can be modified in order to dump data in octal directly from the teletype. The first channel to be printed out may be selected as well as the number of points and the increment between them. The changes to be made are listed below.

A core map for the output routine is also listed.

CORE LOCATION

CORE LOCATION	DEFOSIT
0105	First channel # to be printed out in octal
0106	<pre># of points to be printed out in octal</pre>
3205	1106 / TAD 106
3206	7000 / NOP
3211	1105 / TAD 105
3357	4020 / JMS 20
/ Subroutine to increment char	nnel # by INCREMENT
20	0000
21	1111 / TAD WA
22	1025 / TAD INCREMENT
23	3111 / DCA WA

DEPOSIT

24	5420 / JMP I 20
25	INCREMENT # in octal

DEFAULT

0105	0000
0106	0000
0025	0001

To dump data from the memory of the Nicolet 1074 interfaced to a PDP8-E, halt the program, load address 3200 and depress switches 10 and 11. Then depress start on PDP8-E and computer control on the NICOLET 1074.

FFT MAP

0 - 4	
5 - 7	FLOATING POINT POINTERS
10 - 37	20-25 USED BY OUT PUT ROUTINE
40 - 64	USED BY FLOATING POINT PACKAGE
65 - 67	
70 - 77	FFT SUBROUTINE POINTERS
	USED BY FFT PROGRAM
103 - 106	105-106 USED BY OUT PUT ROUTINE
107 - 177	USED BY FFT PROGRAM
200 - 362	SORT, PASS ONE, and BIT INVERT
365 - 374	INITIALIZE 1070
400 - 447	FLOATING POINT GET
	FLOATING POINT PUT
	GET WITH FIXED TO FLOATING POINT CONVERSION
	GET PROPER PAIR SUBROUTINE
	PUT PROPER PAIR SUBROUTINE
	DATA CHECK ROUTINE
725 - 747	
	INCREMENT PROPER PAIR INDEX
	FFT EXECUTIVE PROGRAM
	FFT MAIN PROGRAM
1255 - 1372	FFT DISPLAY SUBROUTINES
1400 - 1457	
1460 - 1504	
	CHANGE ANGLE SUBROUTINE
1600 - 1770	MULTIPLICATION BY COMPLEX WEIGHTS SUBROUTINE
2000 - 2132	ORDER SUBROUTINE
· ·	FIXED-FLOATING POINT CONVERSION
	PHASE CORRECTION SUBROUTINE
2340 - 2377	CONSTANT'S STORAGE
2400 - 2577	
2600 - 2777	
3000 - 3135	DATA SORT SUBROUTINE
3142 - 3174	DFLOAT SUBROUTINE
3200 - 3375	FFT INPUT-OUTPUT PROGRAM
3400 - 5377	FFT SINE LOOKUP TABLE
5400 - 5577	SINE & COSINE SUBROUTINES
5600 - 7577	FLOATING POINT PACKAGE #1

WITH ADDRESSES:

 6547_8 set to 5400_8 6550_8 set to 5503_8

DESCRIPTION OF THE MODIFICATION RELAX 2 IN ORDER TO DUMP DATA

The data output portion of RELAX 2, a program written by David
Wright of Michigan State University for computer controlled timing and
data aquisition for two pulse experiments was slightly modified in order
to dump data from the Nicolet 1083 computer. The modifications made
were

CORE LOCATION	DEPOSIT
1326	3001332 JMS OCTOUT (Print X)
1327	1330 JMP to 1330 (Y value)
1331	1335 (Forget Dwell)
1332	5051 (Address of OCTOUT)
1337	3001332 JMS OCTOUT (Print Y)

DESCRIPTION OF PROGRAM CONVERT

Program CONVERT is a computer program to convert data from octal to decimal and order in a form compatible with KINFIT.

PROGRAM CONVERT

```
PROGRAM CONVERT (INPUT=65, OUTPUT=65, PUNCH=65)
    DIMENSION IX(2),IY(2),X(2),Y(2)
  5 READ 100,A,B
    IF(EOF(5LINPUT))999,10
100 FORMAT (2E10.2)
 10 READ 105, (IX(I), IY(I), I=1,2)
    IF(EOF(5LINPUT))5,8
105 FORMAT (2010)
  8 PRINT110, (IX(I), IY(I), I=1,2)
110 FORMAT (1X,2010)
    DO 15 K=1,2
    X(K)=IX(K)
 15 Y(K)=IY(K)
    PRINT 115, (X(K), A, Y(K), B, K=1, 2)
115 FORMAT (2(20X,F10.0,F10.8,F10.0,F10.0))
    PUNCH 116, (X(K), A, Y(K), B, K=1, 2)
116 FORMAT(2(F10.0,F10.8,F10.0,F10.0))
    GO TO 10
999 CONTINUE
    END
```

·